

doi: 10.12029/gc20200303001

陶瑞, 海连富, 王磊, 宋扬, 李海峰, 林丽, 梅超, 白金鹤. 2023. 宁夏灵武侏罗系直罗组碎屑岩地球化学特征及源区构造背景分析[J]. 中国地质, 50(6): 1817–1836.

Tao Rui, Hai Lianfu, Wang Lei, Song Yang, Li Haifeng, Lin Li, Mei Chao, Bai Jinhe. 2023. Geochemical characteristics of clastic rocks from the Jurassic Zhiluo Formation in Lingwu, Ningxia and analysis of tectonic background of the source area[J]. Geology in China, 50(6): 1817–1836(in Chinese with English abstract).

## 宁夏灵武侏罗系直罗组碎屑岩地球化学特征及源区构造背景分析

陶瑞<sup>1</sup>, 海连富<sup>1,2</sup>, 王磊<sup>1</sup>, 宋扬<sup>1</sup>, 李海峰<sup>1</sup>, 林丽<sup>3</sup>, 梅超<sup>1</sup>, 白金鹤<sup>1</sup>

(1. 宁夏回族自治区矿产地质调查院(自治区矿产地质研究所), 宁夏 银川 750021; 2. 中国地质大学(武汉)资源学院,  
湖北 武汉 430074; 3. 成都理工大学, 四川 成都 610059)

**摘要:**【研究目的】直罗组在整个侏罗纪演化过程中处于湖进与湖退序列的转换时期, 其构造背景对研究鄂尔多斯盆地西缘断褶带发育的启动时限意义重大。【研究方法】本文采用 XRF 和 ICP-MS 对宁夏灵武侏罗系直罗组 16 件碎屑岩样品进行了主微量元素及稀土元素测试分析, 旨在揭示灵武直罗组碎屑岩地球化学特征及源区构造背景。【研究成果】主量元素间相关系数较低, 微量元素及稀土元素自身相关系数较高,  $\text{Al}_2\text{O}_3$  与微量元素 Co、Ni、Cr、V、Sc、Li、Cs、Be、Ga、Tl、Cu、Pb、Zn、Sn 等元素之间相关系数多大于 0.9,  $\text{TiO}_2$  与 Nb 之间的相关系数为 0.98, 整体显示了沉积物源以陆源碎屑为主; 富集集中型 ( $K > 1, C_v > 1$ ) 元素有 Zr、U、CaO 元素; 富集分散型 ( $K > 1, C_v < 1$ ) 元素有  $\text{Al}_2\text{O}_3$ 、 $\text{Fe}_2\text{O}_3$ 、 $\text{MgO}$ 、Sr、Ba、U、Co、V、Sc、Li、Pb; 贫乏分散型 ( $K < 1, C_v < 1$ ) 元素有  $\text{SiO}_2$ 、 $\text{TiO}_2$ 、 $\text{MnO}$ 、 $\text{Na}_2\text{O}$ 、 $\text{K}_2\text{O}$ 、 $\text{P}_2\text{O}_5$ 、Rb、Th、Nb、Ta、Ni、Cr、Cs、Be、Ga、Tl、Cu、Zn、As、Sn 及稀土元素; 缺乏贫乏集中型 ( $K < 1, C_v > 1$ ) 元素。【结论】主量元素特征氧化物组合的平均值  $\text{TiO}_2$  (0.54)、 $\text{TFe}_2\text{O}_3 + \text{MgO}$  (4.58)、 $\text{Al}_2\text{O}_3/\text{SiO}_2$  (0.18) 与活动大陆边缘相似, 微量元素蛛网图显示直罗组岩石富集 Rb、K、U 等大离子亲石元素, 强烈亏损 Nb、Sr、P、Ti, 稀土元素球粒陨石标准化配分曲线总体表现为轻稀土富集, 重稀土相对亏损的平缓右倾模式, 泥岩 CIA (70.76~81.88), 砂岩 ICV (1.02~1.6) > 泥岩 ICV (0.7~1.14), 泥岩 ICV 基本小于或等于 1, 指示灵武直罗组没有或经历了很弱的再旋回作用, 属于构造活动背景下的初次沉积, 分化程度中等。地球化学特征表明灵武直罗组源区构造背景主要与活动大陆边缘相关, 与大陆岛弧也有较多联系, 总体显示为活动大陆边缘或活动陆缘消减带, 而且可能为安第斯型活动大陆边缘。

**关 键 词:**侏罗系; 直罗组; 碎屑岩地球化学; 构造背景; 地质调查工程; 灵武; 宁夏

**创 新 点:**利用碎屑岩地球化学特征分析了宁夏灵武地区侏罗系直罗组沉积物源特征, 探讨了研究区直罗组源区沉积构造背景。

中图分类号: P581 文献标志码: A 文章编号: 1000-3657(2023)06-1817-20

## Geochemical characteristics of clastic rocks from the Jurassic Zhiluo Formation in Lingwu, Ningxia and analysis of tectonic background of the source area

TAO Rui<sup>1</sup>, HAI Lianfu<sup>1,2</sup>, WANG Lei<sup>1</sup>, SONG Yang<sup>1</sup>, LI Haifeng<sup>1</sup>, LIN Li<sup>3</sup>, MEI Chao<sup>1</sup>, BAI Jinhe<sup>1</sup>

收稿日期: 2020-03-03; 改回日期: 2020-06-03

基金项目: 宁夏自然科学基金项目(2021AAC03446)与宁夏优秀人才支持计划(JTGC2019023)联合资助。

作者简介: 陶瑞, 男, 1990 年生, 博士, 主要从事地质矿产调查与岩石学研究工作; E-mail: 18384127744@163.com。

通讯作者: 海连富, 男, 1989 年生, 博士生, 主要从事地质矿产调查工作; E-mail: 791128985@qq.com。

(1. Ningxia Institute of Mineral Geological Survey (Autonomous Region Institute of Mineral Geology), Yinchuan 750021, Ningxia, China; 2. College of Resources China University of Geosciences (Wuhan), Wuhan 430074, Hubei, China; 3. Chengdu University of Technology, Chengdu 610059, Sichuan, China)

**Abstract:** This paper is the result of geological survey engineering.

**[Objective]** The Zhiluo Formation represents a transitional phase in the lake's advancement and retreat within the broader context of Jurassic geological evolution. Its tectonic background holds paramount importance in exploring the inception timeline of fault–fold belt development along the western margin of the Ordos Basin. This study focuses on the Zhiluo Formation, specifically clastic rocks, from the Jurassic period in the Lingwu area, Ningxia. **[Methods]** We conducted analyses using X–ray and ICP–MS techniques to uncover the geochemical characteristics of clastic rocks and the structural context of the source region. **[Results]** Our results reveal that major element correlation coefficients are generally low, while trace elements and REE exhibit high values. Notably, correlation coefficients between  $\text{Al}_2\text{O}_3$  and trace elements such as Co, Ni, Cr, V, Sc, Li, Cs, Be, Ga, Tl, Cu, Pb, Zn, and Sn exceed 0.9, and the correlation coefficients between  $\text{TiO}_2$  and Nb are at 0.98. This suggests that the primary source of sediment is terrigenous clastic material. Enrichment concentration–type elements ( $K>1, C_V>1$ ) include Zr, U, and CaO, while enrichment dispersion–type elements ( $K>1, C_V<1$ ) consist of  $\text{Al}_2\text{O}_3$ ,  $\text{Fe}_2\text{O}_3$ , MgO, Sr, Ba, U, Co, V, Sc, Li, and Pb. Poorly dispersive elements ( $K<1, C_V<1$ ) encompass  $\text{SiO}_2$ ,  $\text{TiO}_2$ , MnO,  $\text{Na}_2\text{O}$ ,  $\text{K}_2\text{O}$ ,  $\text{P}_2\text{O}_5$ , Rb, Th, Nb, Ta, Ni, Cr, Cs, Be, Ga, Tl, Cu, Zn, As, Sn, and REE. No elements fall under the poor concentration type ( $K<1, C_V>1$ ). **[Conclusions]** The average values for key oxide combinations of main elements are  $\text{TiO}_2$  (0.54),  $\text{TiO}_2+\text{MgO}$  (4.58),  $\text{Al}_2\text{O}_3/\text{SiO}_2$  (0.58), and  $\text{Al}_2\text{O}_3/\text{SiO}_2$  (0.18), indicating similarity to an active continental margin. A trace element spider diagram demonstrates the rocks of the Zhiluo Formation's richness in Rb, K, and U, which are large ion lithophile elements, and a significant deficit in Nb, Sr, P, and Ti. The chondrite–standardized REE distribution curve depicts a gentle right–leaning pattern, signifying LREE enrichment and HREE relative depletion. In terms of geochemical indices, the CIA (70.76–81.88) for mudstone exceeds the ICV (1.02–1.6) for sandstone, while mudstone ICV (0.7–1.14) remains mostly less than or equal to 1. This suggests that the Zhiluo Formation in the Lingwu area exhibits little to no recycling and is characteristic of primary sedimentation in the context of tectonic activity with a moderate degree of differentiation. Correlation diagrams indicates that tectonic background of the source region is primarily associated with an active continental margin. Additionally, it exhibits some links to continental island arc systems, suggesting an active continental margin or an active continental margin subduction zone, potentially resembling an Andean–type active continental margin.

**Key words:** Jurassic; Zhiluo Formation; geochemistry of clastic rocks; tectonic background; geological survey engineering; Lingwu; Ningxia

**Highlights:** The geochemical characteristics of clastic rocks were used to analyze the primary source of sediment characteristics of the Jurassic Zhiluo Formation in the Lingwu area of Ningxia, and the sedimentary structural background of the Zhiluo Formation source area in the study area was explored.

**About the first author:** TAO Rui, male, born in 1990, Ph.D., mainly engaged in geological mineral survey and petrology research; E-mail: 18384127744163@.com.

**About the corresponding author:** HAI Lianfu, male, born in 1989, Ph.D. candidate, mainly engaged in geological and mineral survey; E-mail: 791128985@qq.com.

**Fund support:** Supported by the projects of Ningxia Natural Science Foundation (No.2021AAC03446) and the Ningxia Excellent Talent Support Program (No.JTGC2019023).

## 1 引言

直罗组建组剖面位于陕西富县直罗镇附近。典型剖面有位于内蒙古阿拉善左旗的木葫芦沟剖面及双圈子剖面、固原炭山石岘子北剖面(宁夏回

族自治区地质调查院,2017)。出露岩性以灰绿—黄灰色长石石英砂岩、长石砂岩、粉砂岩、泥岩为主,含植物、孢粉及恐龙化石。目前对直罗组的研究范围以鄂尔多斯盆地东北部为主(雷开宇,2016;张龙等,2016;孙立新等,2017;Jin et al., 2020;张云

等,2022)。研究方向主要为化石及古气候研究(孙立新等,2017)、沉积物源研究(雷开宇,2016;张龙等,2016)、沉积特征研究(赵俊峰等,2010;赵蕾,2011;薛锐等,2017)、地球化学特征与铀矿的关系研究(张天福等,2016;张字龙等,2016)、岩石学特征与铀矿的关系(易超等,2014)、直罗组中铀矿的赋存形式(陈印等,2017)、沉积相研究(缪宗利等,2018)等。直罗组中铀矿研究成果丰富,张字龙等(2008)研究认为,东胜地区直罗组砂体具有很强的还原能力及遭受强烈的后生改造,铀矿成矿潜力较大;郭虎等(2019)对鄂尔多斯盆地黄陵地区直罗组研究发现,该区域直罗组砂岩中铀的富集与硒元素的含量正相关;赵华雷等(2018)研究鄂尔多斯盆地纳岭沟地区直罗组砂岩黏土矿物特征认为铀的富集与黏土矿物的类型及含量有关;杨君等(2019)研究发现直罗组早期主要发育辫状河沉积,是铀矿的有利富集部位;张艳和易超(2017)利用最优化测井解释物性反演方法对直罗组进行研究发现,其下段渗透率和孔隙度利于铀矿的渗流、储集以及后期地浸开采。

侏罗纪与白垩纪之交是燕山运动发育的主要时期,但关于燕山运动的起始时限、发展过程一直存在争议,直罗组在整个侏罗纪演化过程中处于湖进与湖退序列的转换时期,其构造背景是否孕育着鄂尔多斯盆地西缘断褶带发育的启动时限,具有重要的研究意义。宁夏灵武地区位于鄂尔多斯西缘断褶带的前缘,源-汇系统的演化过程演绎了西缘断褶带侏罗纪的构造背景,但由于露头程度较差,制约了侏罗纪岩相古地理的恢复,通过碎屑岩的地球化学特征来反映源区的构造背景是一种相对较好的方法,具有较好的借鉴意义。

沉积岩很好地记录了源岩的成分、物源区古化学风化条件、源区构造背景等方面的信息(龙晓平等,2008)。砂岩的化学组成受物源区制约,能真实地反映物源区的性质及沉积盆地的构造背景(赵英利,2010;赵英利等,2012;吴素娟等,2016)。众多学者利用砂岩的地球化学特征来研究区域大地构造背景及物源区性质,总结了多种构造背景下砂岩主、微量元素地球化学特征(Bhatia, 1983, 1985; Bhatia and Crook, 1986; Roser and Korsch, 1986, 1988; McLennan and Taylor, 1991; McLennan et al.,

1993)。砂岩在沉积盆地古环境、年代学及矿床岩石地球化学等相关领域研究效果显著(李志明等,2003;苏本勋等,2006;柏道远等,2007;何景文等,2015;徐大良等,2016;宋芳等,2016)。泥岩具有显著的粒度均一性、沉积期后不渗透性及微量元素丰度较高等优势,最适合用来追溯物源区性质和判别其构造背景(Condie, 1993)。

目前对直罗组源区构造背景的认识总体上还是以活动大陆边缘背景为主,局部为大陆岛弧背景(吴兆剑等,2013;张天福等,2016;张宾等,2020)。宁夏地区直罗组的研究相对较少,仅罗伟等(2016)对六盘山—贺兰山地区直罗组地球化学特征进行了研究,探讨了六盘山—贺兰山地区直罗组地层分化程度及沉积构造背景(大陆岛弧为主),对其沉积物源及沉积边界进行了限定。笔者通过对宁夏灵武地区直罗组中16件样品进行主、微量及稀土元素地球化学测试分析,探讨了宁夏灵武地区直罗组地球化学特征及源区构造背景。

## 2 研究区地质概况

宁夏灵武位于柴达木—华北板块中南部,地处华北陆块之鄂尔多斯地块西缘、阿拉善微陆块东南部和祁连早古生代造山带东北缘。邻区是连接中国北方东西部不同大地构造单元的枢纽地区,亦是中国地层、岩相古地理、构造、地貌以及重力、航磁等各种地球物理场的重要分界区域。研究区位于鄂尔多斯地块西缘逆冲带中段(图1),夹持于黄河断裂与车道—阿色浪断裂之间,褶皱及断层构造发育,主要有鸳鸯湖背斜、磁窑堡向斜;断层以逆断层为主。第四纪地貌为冲(湖)积拉张型断陷平原及干燥剥蚀台地。区内未见岩浆活动,地层分区属华北地层区、鄂尔多斯西缘地层分区之卓子山—青龙山地层小区(宁夏回族自治区地质调查院,2017)。

研究区构造位置上属于鄂尔多斯盆地西缘逆冲带(图2a),区内第四系覆盖严重,零星出露中三叠统二马营组( $T_{2e}$ )、上三叠统上田组( $T_{3s}$ )、中侏罗统延安组( $J_{2y}$ )和直罗组( $J_{2z}$ )、上侏罗统安定组( $J_{3a}$ )(图2b)。中侏罗统直罗组( $J_{2z}$ )为本次研究的目的层,该组整合于中侏罗统延安组之上,与上覆上侏罗统安定组为连续沉积。直罗组宏观上以灰绿色为代表色,本次研究根据岩性组合将其划分为两

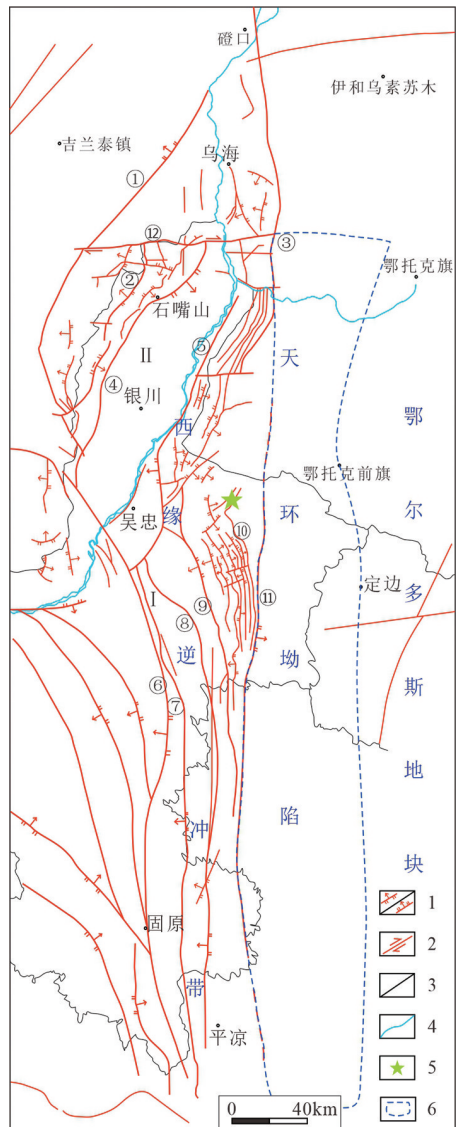


图1 鄂尔多斯盆地西缘构造纲要图(据曹代勇等,2015修编)  
1—逆断层/正断层;2—平移断层;3—省界;4—河流;5—研究区;  
6—构造分区;I—六盘山东麓逆冲推覆构造系统;II—贺兰山逆冲  
推覆构造系统;①—磴口—阿拉善左旗断裂;②—小松山断裂;③—  
卓子山东麓断裂;④—贺兰山东麓断裂;⑤—黄河断裂;⑥—青铜峡—  
固原断裂;⑦—韦州—安国断裂;⑧—青山山—平凉断裂;⑨—惠  
安堡—沙井子断裂;⑩—马柳断裂;⑪—车道—阿色浪断裂;⑫—正  
义关断裂

Fig.1 Structural outline map of the western margin of Ordns Basin (modified from Cao Daiyong et al., 2015)

1—Reverse fault/Normal fault; 2—Translation fault; 3—Provincial boundary; 4—River; 5—Study area; 6—Structural division; I—Thrust nappe structural system at the eastern foot of Liupan Mountain; II—Helan Mountain thrust nappe structural system; ①—Dengkou-Alashan Zuoqi fault; ②—Xiaosongshan fault; ③—Fault at the eastern foot of Zhuozi Mountain; ④—Fault at the eastern foot of Helan Mountain; ⑤—Yellow River fault; ⑥—Qingtongxia—Guyuan fault; ⑦—Weizhou Anguo fault; ⑧—Qinglongshan—Pingliang fault; ⑨—Hui'anpu—Shajingzi fault; ⑩—Maliu fault; ⑪—Chedao—Aselang fault; ⑫—Zhengyiguan fault

段。直罗组二段:上部为灰绿色、紫红色、褐色泥岩、粉砂质泥岩与灰绿色粉砂岩、中细粒岩屑石英砂岩、长石石英砂岩互层。常发育水平层理、平行层理、小型交错层理、板状交错层理、块状层理等,见虫迹;下部为紫红色、浅紫红色、灰白色细粒长石石英砂岩、中粗粒长石石英砂岩、岩屑石英砂岩夹灰绿色块状泥岩、粉砂岩,底部常见河床滞留相砾岩,发育平行层理、槽状交错层理、板状交错层理等沉积构造。直罗组一段:以灰白色、褐灰色、黄绿色中厚层状细粒岩屑石英砂岩、杂砂岩、中粒长石石英砂岩主,夹灰黄色泥页岩。砂岩中常见平行层理、块状层理、槽状交错层理、波状纹层、波痕等,偶见生物扰动痕迹明显,发育虫迹。该段产丰富的植物化石。

### 3 样品采集及测试方法

本次研究共采集新鲜的、受后期成岩作用影响较小的砂岩、泥岩样品16件,主要用于主量、微量及稀土元素分析。其中宁夏灵武直罗组砂岩样品11件,泥岩样品5件。砂岩样品中7件采于灵武市国家地质公园科ZK01钻孔岩心,4件采集于恐龙化石赋存剖面PM01;样品新鲜,质量可以保证物源信息及沉积环境的准确。本次样品的主量、微量和稀土元素测试均在武汉上谱分析科技有限责任公司实验室完成。主量元素采用X射线荧光光谱仪分析;微量元素和稀土元素测试采用等离子体质谱仪(ICP-MS)进行,测试的样品均采用国际标样AGV-2、BHVO-2、BCR-2、BGM-2作为标准,测试结果可靠。

### 4 测试结果

研究区直罗组样品主量元素、微量元素及稀土元素测试结果分别见表1、表2和表3。

#### 4.1 主量元素特征

由表1可知,研究区直罗组砂岩主量元素含量为: $\text{SiO}_2=43.66\% \sim 75.3\%$ 、 $\text{Al}_2\text{O}_3=9.72\% \sim 13.53\%$ 、 $\text{CaO}=0.84\% \sim 19.07\%$ 、 $\text{MgO}=0.7\% \sim 1.42\%$ 、 $\text{TFe}_2\text{O}_3=1.76\% \sim 4.93\%$ 、 $\text{K}_2\text{O}=1.86\% \sim 3.14\%$ 、 $\text{Na}_2\text{O}=1.77\% \sim 2.65\%$ 。 $\text{Al}_2\text{O}_3/\text{SiO}_2=0.15 \sim 0.22$ ,平均值为0.18,与活动大陆边缘(0.15%~0.22)一致。 $\text{TiO}_2=0.29\% \sim 1.25\%$ ,平均0.54%,与活动大陆边缘(0.46%)范围基

表1 灵武直罗组沉积物主量元素含量分析结果(%)

岩性	样品名称	SiO <sub>2</sub>	TiO <sub>2</sub>	Al <sub>2</sub> O <sub>3</sub>	TFe <sub>2</sub> O <sub>3</sub>	MnO	MgO	CaO	Na <sub>2</sub> O	K <sub>2</sub> O	P <sub>2</sub> O <sub>5</sub>	LOI	Total	C	N	P	C*	A	K	CIA	CIA <sub>ion</sub>	ICV
砾岩	科ZK01-10GS1	67.96	0.66	11.59	3.2	0.15	0.89	5.39	2.33	2.32	0.07	5.14	99.7	0.0963	0.0376	0.0005	0.0376	0.1137	0.0246	53.26	55.57	1.34
砾岩	科ZK01-19GS1	43.66	0.44	9.72	5	0.43	1.33	19.07	1.77	1.86	0.06	16.39	99.73	0.3405	0.0285	0.0004	0.0285	0.0953	0.0197	55.41	57.68	1.6
砾岩	科ZK01-23GS1	74.9	0.58	11.61	3.35	0.06	0.87	1.17	2.31	2.65	0.07	2.1	99.67	0.0209	0.0373	0.0005	0.0192	0.1139	0.0281	57.38	61.59	1.19
砾岩	科ZK01-35GS1	71.68	1.25	11.58	4.34	0.11	1.07	2.01	1.87	2.46	0.08	3.25	99.7	0.0359	0.0302	0.0006	0.034	0.1136	0.0261	55.71	58.77	1.42
砾岩	科ZK01-57GS1	72.33	0.49	13.25	3.66	0.05	0.96	0.96	2.65	2.99	0.05	2.19	99.58	0.0171	0.0427	0.0004	0.016	0.13	0.0317	58.98	62.64	1.11
砾岩	科ZK01-64GS1	75.3	0.51	12.4	2.41	0.05	0.78	0.84	2.25	3.13	0.06	2.31	100.04	0.015	0.0363	0.0004	0.0136	0.1216	0.0332	59.4	63.56	1.03
砾岩	科ZK01-70GS1	74.93	0.29	12.6	1.76	0.04	0.7	1.3	2.41	3.14	0.09	2.37	99.63	0.0232	0.0389	0.0006	0.0211	0.1236	0.0333	56.98	62.04	1.02
砾岩	PM01(1)GS1	72.49	0.48	12.59	4.26	0.06	1.19	0.91	2.29	2.79	0.06	2.82	99.94	0.0163	0.0369	0.0004	0.0148	0.1235	0.0296	60.3	64.71	1.17
砾岩	PM01(1)GS2	70.5	0.36	13.31	4.93	0.06	1.42	0.85	2.52	2.8	0.05	2.79	99.59	0.0152	0.0406	0.0004	0.014	0.1305	0.0297	60.75	62.89	1.19
砾岩	PM01(3)GS1	74.03	0.39	12.62	2.68	0.16	1.08	1.07	2.52	2.73	0.07	2.28	99.63	0.0191	0.0406	0.0005	0.0175	0.1238	0.029	58.7	66.24	1.11
砾岩	PM01(4)GS1	71.32	0.51	13.53	3.2	0.16	1.33	1.09	2.5	2.69	0.08	2.84	99.25	0.0195	0.0403	0.0006	0.0176	0.1327	0.0286	60.54	63.91	1.12
平均值		69.92	0.54	12.25	3.53	0.12	1.06	3.15	2.31	2.69	0.07	4.04	99.68	0.0563	0.0373	0.0005	0.0213	0.1202	0.0285	57.95	61.78	1.21
泥岩	科ZK01-5GS1	62.16	0.84	16.79	7.03	0.05	2.37	1.05	1.91	2.5	0.08	4.85	99.63	0.0188	0.0308	0.0006	0.0169	0.1647	0.0265	68.94	70.76	1.14
泥岩	科ZK01-7GS1	60.09	0.93	18.49	7.17	0.05	2.46	0.78	1.65	2.54	0.06	5.67	99.89	0.0139	0.0266	0.0004	0.0125	0.1813	0.027	73.28	75.08	1.02
泥岩	科ZK01-12GS1	57.88	0.97	19.9	7.45	0.07	3.05	0.65	1.54	2.68	0.1	5.79	100.08	0.0116	0.0248	0.0007	0.0093	0.1952	0.0285	75.72	77.56	1.01
泥岩	科ZK01-76GS1	59.94	0.98	21.04	5.22	0.03	1.81	0.42	1.04	2.83	0.04	6.5	99.85	0.0075	0.0168	0.0003	0.0066	0.2064	0.03	79.45	81.88	0.7
泥岩	科ZK01-86GS1	54.64	0.85	20.79	8.44	0.08	2.88	1.04	1.26	2.64	0.11	7.49	100.22	0.0186	0.0203	0.0008	0.016	0.2039	0.028	76.03	77.57	0.98
平均值		58.94	0.91	19.4	7.06	0.06	2.51	0.79	1.48	2.64	0.08	6.06	99.93	0.0141	0.0239	0.0006	0.0123	0.1903	0.028	74.68	76.57	0.97
PAAS		62.8		18.88	7.18		2.19	1.29	1.19	3.69	0.16											

注:PAAS为澳大利亚后太古宙平均页岩(Taylor and McLennan, 1985);CIA为成分变异指数;C\*指硅酸盐矿物中的CaO。

表2 灵武直罗组沉积物微量元素含量分析结果( $10^{-6}$ )  
Table 2 Analytical result ( $10^{-6}$ ) of trace elements in sediments of Zhiluo Formation in Lingwu

岩性	样品名	本相符合。灵武直罗组泥岩主量元素含量为: $\text{SiO}_2=54.64\% \sim 62.16\%$ 、 $\text{Al}_2\text{O}_3=16.79\% \sim 21.04\%$ 、 $\text{CaO}=0.42\% \sim 1.05\%$ 、 $\text{MgO}=1.81\% \sim 2.88\%$ 、 $\text{TFe}_2\text{O}_3=5.22\% \sim 8.44\%$ 、 $\text{K}_2\text{O}=2.5\% \sim 2.83\%$ 、 $\text{Na}_2\text{O}=1.04\% \sim 1.91\%$ , 其平均值分别为 58.94%、19.4%、0.79%、2.51%、7.06%、2.64%、1.48%。																											
		Li	Be	Sc	V	Cr	Co	Ni	Cu	Zn	Ga	Rb	Sr	Y	Zr	Nb	Sn	Cs	Ba	Hf	Ta	Tl	Pb	Th	U	Sr/Ba	Sr/Cu	Rb/Sr	V/(V+Ni)
砂岩	科ZK01-10GS1	15.1	1.21	8.98	38.5	7.44	11.8	8.58	34	13.1	67.6	265	22.4	411	10.3	1.69	1.58	2183	9.22	0.77	0.4	13.8	8.19	1.7	0.12	30.89	0.26	0.83	
	科ZK01-19GS1	21.9	1.69	7.6	53.1	32.4	11.7	16.8	9.99	48.3	12.2	71.8	377	18.1	124	7.13	1.42	2.81	435	3.15	0.49	0.48	12.8	4.94	1.12	0.87	37.74	0.19	0.76
	科ZK01-23GS1	17.1	1.47	7.21	50.1	29.8	6.74	11.2	5.58	36.8	12.4	84.7	217	17.9	187	10.1	1.67	2.04	570	4.71	0.77	0.51	16.1	8.6	1.39	0.38	38.89	0.39	0.82
	科ZK01-35GS1	19.8	1.42	11.3	63.5	45.1	9.16	13.4	6.72	48	13.9	78.7	203	41.1	1859	18.2	2.34	1.9	548	41.8	1.29	0.52	17.2	23.1	6.44	0.37	30.21	0.39	0.83
	科ZK01-57GS1	23	1.65	8.61	49.9	29.2	11.6	13.9	5.82	46.8	14.7	92.9	244	15.2	179	7.94	1.78	2.55	724	4.44	0.58	0.6	18.5	6.57	2.16	0.34	41.92	0.38	0.78
	科ZK01-64GS1	16.6	1.48	6.03	50.3	23.8	10.3	11.5	5.18	38	13.6	94	215	16.3	195	8.49	1.82	2	723	4.82	0.65	0.69	19.1	7.61	5.03	0.3	41.51	0.44	0.81
砂岩	科ZK01-70GS1	18.4	1.47	5.12	39	20.7	8.09	10.1	4.76	31.5	13.5	90.7	243	12.4	97.6	5.4	1.49	1.87	777	2.56	0.4	0.62	17.5	4.59	2.61	0.31	51.05	0.37	0.79
	PM01(1)GS1	23.9	1.74	7.39	53.1	29.1	7.79	11.9	4.83	47.7	13.9	78	255	11.6	171	7.73	1.61	1.82	723	4.27	0.56	0.51	16.6	5.93	2.74	0.35	52.8	0.31	0.82
	PM01(1)GS2	33.1	1.78	7.03	57.2	28.5	8.76	14.8	4.1	58	13.7	81.9	253	9.64	141	6.23	1.54	2.07	717	3.6	0.48	0.54	18.3	5.68	2.94	0.35	61.71	0.32	0.79
	PM01(3)GS1	19.2	1.42	7.21	52	25.8	6.39	16.2	3.96	31.7	13.3	75.4	264	11.1	131	6.32	1.5	1.61	730	3.47	0.49	0.62	13.8	5.61	3.84	0.36	66.67	0.29	0.76
	PM01(4)GS1	34.6	1.65	9.3	44.2	34.3	12.4	18.9	4.39	55.2	14.9	79	259	14.7	171	8.16	1.66	2	689	4.29	0.59	0.69	13.4	6.58	6.88	0.38	59	0.31	0.7
	科ZK01-5GS1	49.5	2.46	15.9	102	65.1	15.2	31.4	23.4	89.9	21.9	111	223	28.3	248	13.7	2.41	5.2	545	6.13	0.93	0.71	19.7	11.8	10.1	0.41	9.53	0.5	0.76
	科ZK01-7GS1	57.4	2.49	17.7	111	81.4	14.9	33.4	26.8	90.2	23.7	115	199	24.3	265	15.4	2.71	6.28	541	6.61	1.05	0.74	23.9	15.4	4.92	0.37	7.43	0.58	0.77
泥岩	科ZK01-12GS1	59.5	2.73	19.4	133	83.8	29.8	53.4	38	107	26	127	165	26	196	16.6	2.99	6.94	501	5.14	1.07	0.77	29.3	16.8	2.92	0.33	4.34	0.77	0.71
	科ZK01-76GS1	60.7	2.9	17.4	123	82	18	39.8	35.6	90.6	27.1	150	182	22.9	206	19	3.38	8.25	465	5.51	1.26	0.9	21.8	18.8	8.16	0.39	5.11	0.82	0.76
	科ZK01-86GS1	61.3	3.4	19.7	139	82.3	16.9	40.4	42.6	101	27.2	128	198	33.1	130	14.5	3.07	8.56	484	3.63	1.01	0.82	32.3	19.9	2.13	0.41	4.65	0.65	0.77

表3 灵武直罗组沉积物稀土元素含量分析结果( $10^{-6}$ )  
Table 3 Analytical result ( $10^{-6}$ ) of rare earth element in sediments of Zhiluo Formation in Lingwu

岩性	样品号	La	Ce	Pr	Nd	Sm	Eu	Gd	Tb	Dy	Ho	Er	Tm	Yb	Lu	$\Sigma$ REE	LREE	HREE	$(\text{La/Yb})_{\text{n}}$	$\delta\text{Eu}$	$\delta\text{Ce}$	$\text{Ce}_{\text{anom}}$	
科ZK01-10GS1	32.5	67.1	7.63	28.5	5.33	1.08	4.31	0.66	4	0.8	2.29	0.36	2.28	0.37	157.21	142.14	15.07	9.43	1.34	1.06	1.01	-0.01	
科ZK01-19GS1	23.2	46.1	5.1	19.4	3.59	0.87	3.44	0.47	3.03	0.6	1.77	0.26	1.69	0.27	109.79	98.26	11.53	8.52	1.29	1.16	1.01	-0.03	
科ZK01-23GS1	28.5	60.1	6.84	25.4	4.6	1.02	3.84	0.54	3.33	0.62	1.8	0.26	1.79	0.28	138.92	126.46	12.46	10.15	1.5	1.14	1.02	-0.01	
科ZK01-35GS1	60.9	137	13.9	51.4	8.91	1.3	7.33	1.08	6.89	1.4	4.41	0.72	5.01	0.81	301.06	273.41	27.65	9.89	1.15	0.76	1.12	0.03	
科ZK01-57GS1	29.8	62.4	6.73	25.3	4.56	1.06	3.5	0.55	2.85	0.51	1.49	0.22	1.41	0.22	140.6	129.85	10.75	12.08	1.99	1.25	1.05	0	
砂岩	科ZK01-64GS1	27.5	58.7	6.36	23.5	4.22	0.92	3.17	0.52	2.8	0.53	1.6	0.24	1.51	0.25	131.82	121.2	10.62	11.41	1.72	1.18	1.05	0
科ZK01-70GS1	22.8	47.4	4.99	18.7	3.25	0.85	2.64	0.43	2.26	0.44	1.3	0.18	1.24	0.19	106.67	97.99	8.68	11.29	1.73	1.36	1.05	0	
PM01(1)GS1	22.7	49.1	5.26	19.2	3.44	0.85	2.64	0.43	2.36	0.44	1.35	0.21	1.4	0.21	109.59	100.55	9.04	11.12	1.53	1.32	1.07	0.01	
PM01(1)GS2	18.6	44.7	4.48	16.7	3.04	0.75	2.3	0.37	2.05	0.39	1.13	0.17	1.11	0.17	95.96	88.27	7.69	11.48	1.58	1.33	1.16	0.05	
PM01(3)GS1	28.1	60.8	6.02	21.6	3.53	0.83	2.67	0.42	2.17	0.41	1.18	0.18	1.19	0.18	129.28	120.88	8.4	14.39	2.23	1.27	1.11	0.02	
PM01(4)GS1	31.5	62.1	6.61	24.5	4.03	0.93	3.24	0.5	2.68	0.52	1.48	0.23	1.47	0.22	140.01	129.67	10.34	12.54	2.02	1.21	1.02	-0.02	
科ZK01-5GS1	42.3	83.6	9.88	37.2	6.8	1.46	5.89	0.89	5.36	1.03	2.94	0.44	2.76	0.43	200.98	181.24	19.74	9.18	1.45	1.08	0.97	-0.03	
科ZK01-7GS1	41.4	81.8	9.23	33.8	6.14	1.28	5.1	0.75	4.61	0.9	2.62	0.41	2.82	0.42	191.28	173.65	17.63	9.85	1.38	1.07	0.99	-0.02	
泥岩	科ZK01-12GS1	48	96.5	10.7	39	6.86	1.39	5.45	0.79	4.7	0.94	2.83	0.41	2.7	0.43	220.7	202.45	18.25	11.09	1.68	1.07	1.01	-0.01
科ZK01-76GS1	39.3	77.1	8.44	30.1	5.09	0.98	3.77	0.67	3.85	0.78	2.46	0.38	2.71	0.39	176.02	161.01	15.01	10.73	1.37	1.05	1	-0.02	
科ZK01-86GS1	49.3	100	11.1	41.2	7.79	1.6	6.24	1.02	6.03	1.19	3.37	0.49	3.11	0.44	232.88	210.99	21.89	9.64	1.49	1.08	1.01	-0.02	
北美页岩	(Gromet et al., 1984)	31.5	66.5	7.9	27	5.9	1.18	5.2	0.79	5.8	1.04	3.4	0.5	2.97	0.44								

注:  $\text{Ce}_{\text{anom}} = \lg[\text{Ce}_{\text{La}} / (\text{La}_{\text{N}} + \text{Nd}_{\text{D}})]$

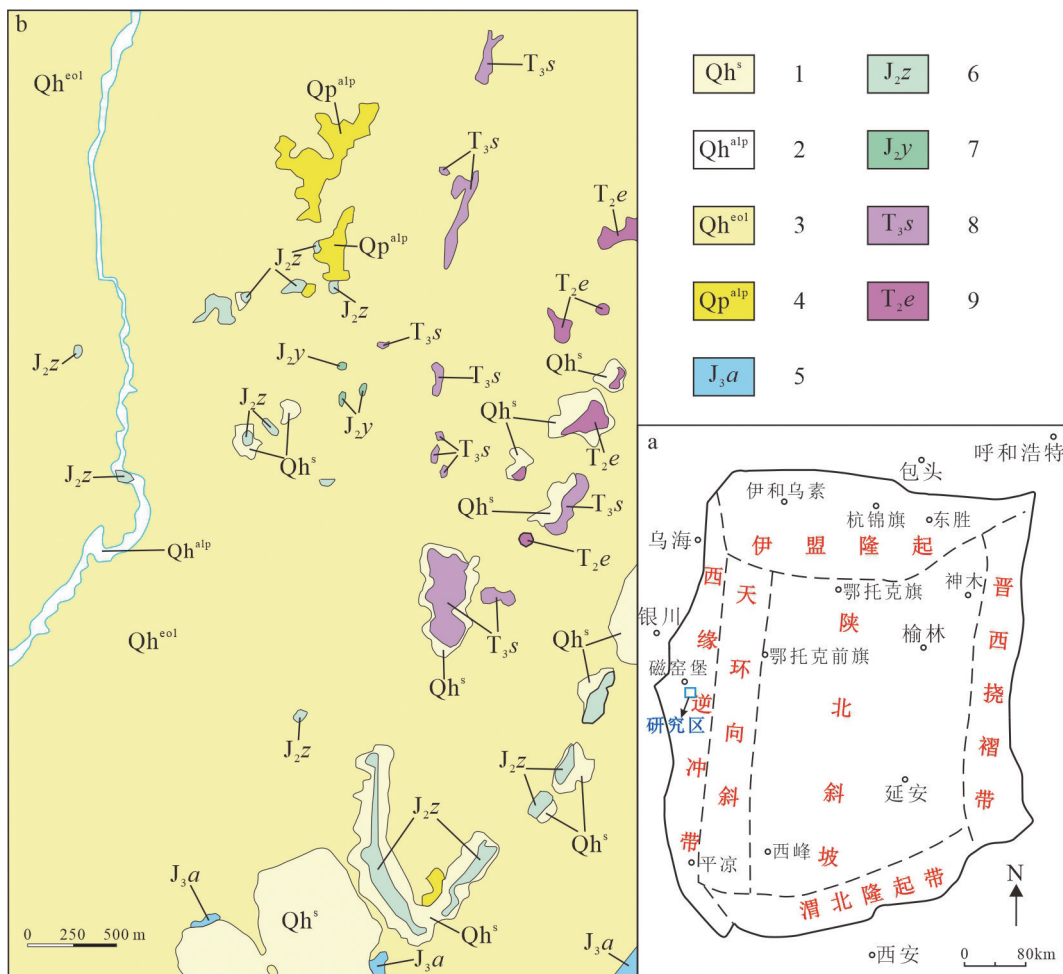


图2 研究区构造位置图(a)与地质简图(b)

1—全新统人工堆积;2—全新统冲积洪积;3—全新统风成沙;4—更新统冲积洪积;5—上侏罗统安定组;6—中侏罗统直罗组;7—中侏罗统延安组;8—上三叠统上田组;9—中三叠统二马营组

Fig.2 Tectonic map (a) and simplifield geological map (b) in the study area

1—Holocene artificial accumulation; 2—Holocene alluvial proluvial; 3—Holocene eolian sand; 4—Pleistocene alluvial proluvial; 5—Upper Jurassic Anding Formation; 6—Middle Jurassic Zhiluo Formation; 7—Middle Jurassic Yan'an Formation; 8—Upper Triassic Shangtian Formation; 9—Middle Triassic Ermaying Formation

稀土元素相对亏损且曲线较为平缓。同时研究区直罗组砂岩稀土元素球粒陨石标准化配分曲线具有明显的特点( $\delta Eu=0.76\sim1.36$ , 均值1.19),以上特点与活动大陆边缘物源区的沉积岩稀土元素配分特点相似(Bhatia, 1985)。 $\delta Eu$ 的变化取决于碎屑物源的组成, $Eu$ 具弱负异常,指示其源岩与花岗岩类等酸性岩及上地壳相关。在北美页岩标准化配分模式图(图4b)中,直罗组砂岩表现出较为平坦的曲线,出现较强的Eu正异常。

研究区直罗组泥岩稀土元素总量 $\Sigma REE=176.02\times10^{-6}\sim232.88\times10^{-6}$ (表3), $\Sigma LREE/\Sigma HREE$ 值

在9.18~11.09,(La/Yb)<sub>N</sub>(北美页岩标准化)在1.37~1.68。在稀土元素球粒陨石标准化配分模式图(图4c)中,直罗组泥岩显示出较高的(La/Yb)<sub>N</sub>,Eu负异常。在北美页岩标准化稀土元素配分图解中(图4d),直罗组泥岩表现出较为平坦的曲线,无Eu异常或弱的Eu正异常。

#### 4.4 元素地球化学基本特征分析

##### 4.4.1 元素相关性分析

各元素相关系数(表4)显示,研究区直罗组主量元素之间相关系数较低,但 $Al_2O_3$ 、 $Fe_2O_3$ 、 $MgO$ 与微量元素 $Co$ 、 $Ni$ 、 $Cr$ 、 $V$ 、 $Sc$ 、 $Li$ 、 $Cs$ 、 $Be$ 、 $Ga$ 、 $Tl$ 、 $Cu$ 、 $Pb$ 、 $Zn$ 、 $Sn$ 等元素之间相关系数较高,介于0.51~

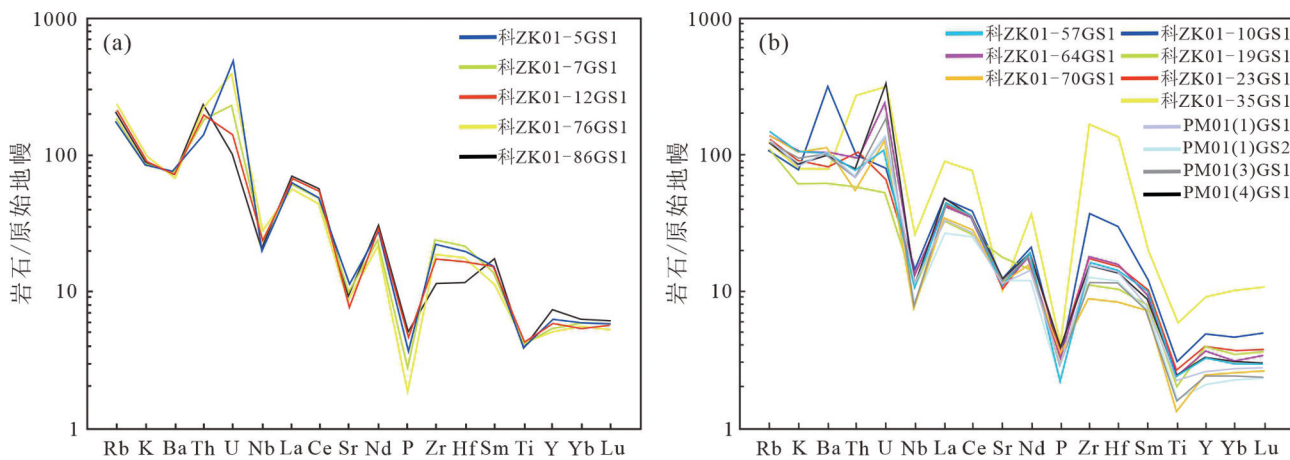


图3 灵武直罗组泥岩(a)和砂岩(b)微量元素原始地幔标准化蛛网图(标准化值据 Sun and McDonough, 1989)  
Fig.3 Primitive mantle-normalized spider diagrams of the mudstone (a) and sandstone (b) from Zhi Luo Formation in Lingwu  
(normalized values are from Sun and McDonough, 1989)

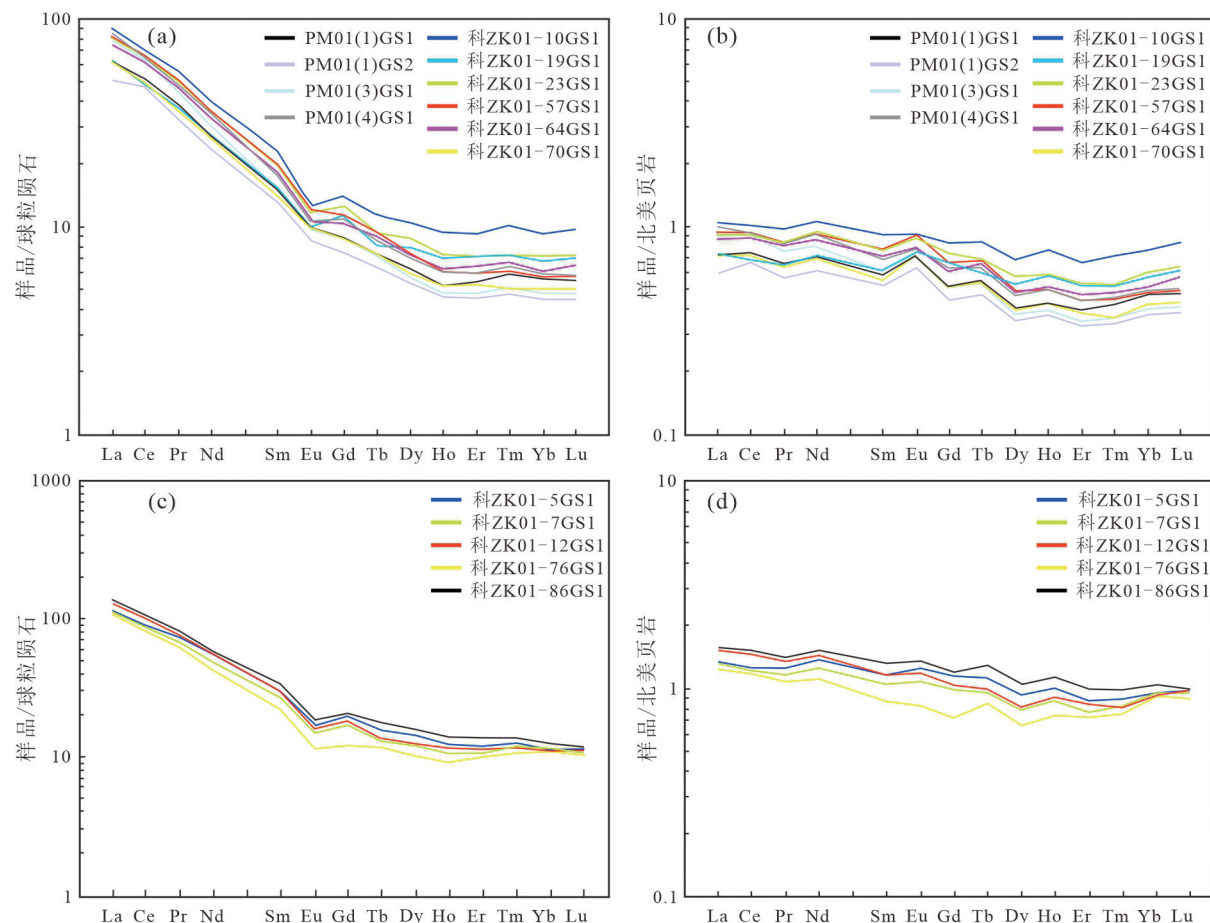


图4 灵武直罗组砂岩、泥岩稀土元素球粒陨石标准化配分图(a、c)与北美页岩标准化配分模式图(b、d)(球粒陨石标准化值据 Sun and McDonough, 1989; 北美页岩标准化值据 Gromet et al., 1984)  
Fig.4 Chondrite-normalized rare earth elements patterns (a, c) and NASC (North American shale composite)-normalized rare earth elements patterns (b, d) of the sandstone and mudstone from Zhi Luo Formation in Lingwu (Chondrite-normalized values are from Sun and McDonough, 1989; NASC-normalized values are from Gromet et al., 1984)

表 4 灵武直罗组沉积物主量、微量元素、稀土元素相关性分析结果  
Table 4 Characteristic element parameters of major, trace and REEs in sediments of Zhiluo Formation in Lingwu

表5 灵武直罗组沉积物稀土元素相关性分析结果

Table 5 Correlation analysis results of REEs in sediments of Zhiluo Formation, Lingwu

元素	La	Ce	Pr	Nd	Sm	Eu	Gd	Tb	Dy	Ho	Er	Tm	Yb	Lu	Y
La	1														
Ce	0.9862	1													
Pr	0.9946	0.9878	1												
Nd	0.9908	0.9848	0.9989	1											
Sm	0.9727	0.9624	0.988	0.9924	1										
Eu	0.8515	0.7944	0.867	0.8764	0.9137	1									
Gd	0.9478	0.934	0.9665	0.9755	0.9885	0.9144	1								
Tb	0.957	0.9383	0.9707	0.9767	0.9904	0.9221	0.9832	1							
Dy	0.9452	0.932	0.9633	0.9705	0.9854	0.8978	0.9914	0.9916	1						
Ho	0.9487	0.9372	0.9639	0.9697	0.9811	0.8781	0.9859	0.987	0.9979	1					
Er	0.9548	0.9522	0.9681	0.9717	0.9741	0.8358	0.9744	0.9749	0.9889	0.9945	1				
Tm	0.9477	0.955	0.9608	0.9635	0.9595	0.7881	0.9584	0.9567	0.9746	0.9824	0.9944	1			
Yb	0.9395	0.9525	0.9497	0.9496	0.9378	0.7409	0.9338	0.931	0.9529	0.9635	0.9839	0.9949	1		
Lu	0.9223	0.9451	0.9371	0.9388	0.9244	0.7085	0.9249	0.9091	0.9367	0.948	0.9727	0.9883	0.9939	1	
Y	0.9463	0.9388	0.9601	0.9661	0.9736	0.8488	0.9785	0.9789	0.9913	0.9947	0.9951	0.9859	0.9702	0.9591	1

0.96,且多大于0.9,TiO<sub>2</sub>与Nb之间的相关系数为0.98,整体显示了沉积物源以陆源碎屑为主;微量元素Rb、Co、Ni、Cr、V、Sc、Li、Cs、Be、Ga、Tl、Cu、Pb、Zn等元素之间相关系数较高,均在0.69以上,其中Ga、Cu、Zn与其余元素相关系数均在0.9以上,具强烈正相关关系,Th、Nb、Ta与稀土元素相关系数均在0.8以上,具明显正相关关系;稀土元素之间相关系数均在0.7以上,大多数大于0.9(表5)。而CaO、Na<sub>2</sub>O、K<sub>2</sub>O、Sr、Ba、As与其他多数元素相关系数小于0,无明显相关关系(表4)。

#### 4.4.2 元素富集特征

研究区直罗组各元素特征参数统计表(表6)显示,明显富集的元素为U、Fe<sub>2</sub>O<sub>3</sub>,富集系数K=1.77~1.91;Al<sub>2</sub>O<sub>3</sub>、MgO、V、Sr、Sc、Ba、Co、Hf、CaO、Li、Zr、Pb元素弱富集,富集系数1.0< K < 1.5;Be、Cu、Rb、Ni、Zn、Ga、SiO<sub>2</sub>、Th、Tl、Y、Sn、Cr、La、Ce、Pr、Nd、Sm、Eu、Gd、Yb、Lu表现为略贫乏,富集系数为0.8< K < 1;表现为较贫乏的元素为TiO<sub>2</sub>、Ho、Na<sub>2</sub>O、As、Nb、Er、Dy、Ta、Tm、Cs、Tb、K<sub>2</sub>O,富集系数0.5< K < 0.8;表现为贫乏的元素为MnO、P<sub>2</sub>O<sub>5</sub>,富集系数K<0.5。富集系数排序图(图5)显示的特征与之相同。

#### 4.4.3 元素变异特征

灵武直罗组沉积物元素变异系数排序图(图6)显示,元素的变异系数总体都不高,除了CaO变异系数( $C_V$ )(表6)1.9外,其余都在1.5以下,从大到小排列顺序为:CaO、Zr、Hf、MnO、Cu、Cs、U、Ni、Ba、Th、Li、Cr、MgO、Co、Lu、Yb、V、Sc、Tm、Zn、Fe<sub>2</sub>O<sub>3</sub>、Er、Y、TiO<sub>2</sub>、Nb、Ho、Dy、Ta、Gd、Ce、Sm、Tb、La、Pr、Nd、Be、Ga、Sn、Pb、P<sub>2</sub>O<sub>5</sub>、Al<sub>2</sub>O<sub>3</sub>、Rb、Na<sub>2</sub>O、Eu、Tl、Sr、As、SiO<sub>2</sub>、K<sub>2</sub>O。

各元素特征参数统计表(表6)显示,强变异( $C_V > 1.0$ )的有Zr、U、CaO元素,表明其呈明显的不均匀分布,同时富集程度较高,其中CaO变异系数最大,为1.9。变异系数(0.5< $C_V$ <1.0)的有MgO、Cr、Li、Ba、Th、Ni、U、Cs、Cu、MnO等元素,一般为不均匀分布,同时富集程度较低。弱变异( $C_V < 0.5$ )的元素有K<sub>2</sub>O、SiO<sub>2</sub>、As、Sr、Tl、Na<sub>2</sub>O、Eu、Al<sub>2</sub>O<sub>3</sub>、Rb、P<sub>2</sub>O<sub>5</sub>、Pb、Sn、Be、Ga、La、Pr、Nd、Ce、Sm、Tb、Gd、Ta、Dy、TiO<sub>2</sub>、Nb、Ho、Fe<sub>2</sub>O<sub>3</sub>、Er、Y、Zn、Tm、V、Sc、Yb、Co、Lu等元素,分布也不均匀,仅具有分散特征。

总体而言,属于富集集中型( $K > 1$ 、 $C_V > 1$ )的元素有Zr、U、CaO元素(图7);属于富集分散型( $K > 1$ 、 $C_V < 1$ )的元素有Al<sub>2</sub>O<sub>3</sub>、Fe<sub>2</sub>O<sub>3</sub>、MgO、Sr、Ba、U、Co、V、

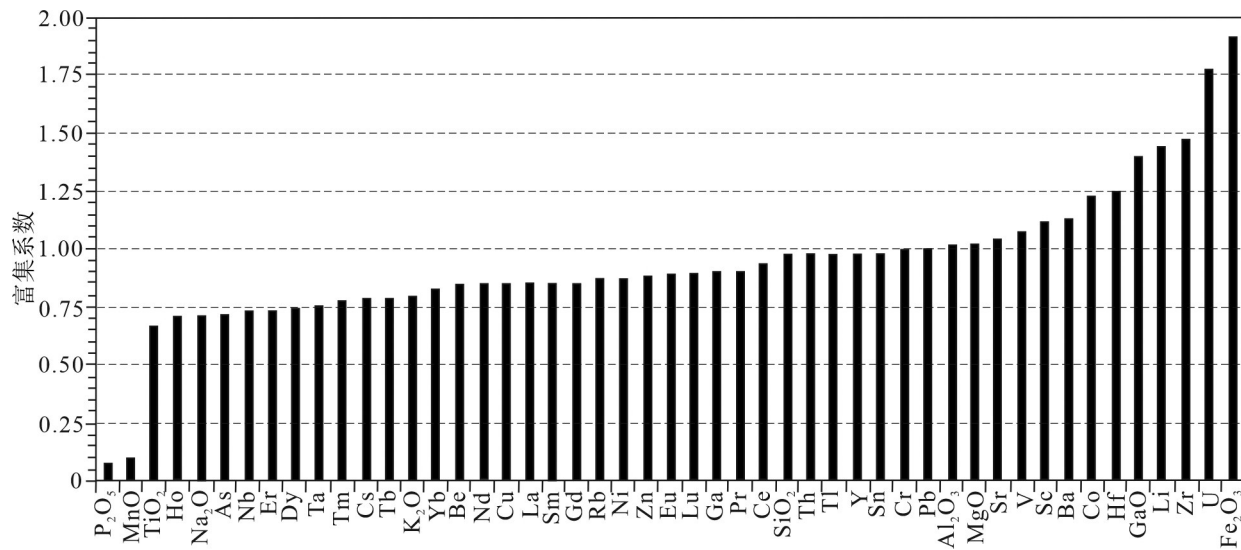


图5 灵武直罗组沉积物元素富集系数排序图

Fig.5 Sequence diagram of element enrichment coefficient in sediments of Zhiluo Formation in Lingwu

Sc、Li、Pb；属于贫乏分散型( $K<1$ 、 $C_V<1$ )的元素有SiO<sub>2</sub>、TiO<sub>2</sub>、MnO、Na<sub>2</sub>O、K<sub>2</sub>O、P<sub>2</sub>O<sub>5</sub>、Rb、Th、Nb、Ta、Ni、Cr、Cs、Be、Ga、Tl、Cu、Zn、As、Sn及稀土元素；缺乏贫乏集中型( $K<1$ 、 $C_V>1$ )的元素。

## 5 源区构造背景讨论

Bhatia(1983)通过大量研究澳大利亚东部不同构造背景下砂岩的主量元素特征,认为主量元素SiO<sub>2</sub>、TiO<sub>2</sub>、TFe<sub>2</sub>O<sub>3</sub>+MgO、Al<sub>2</sub>O<sub>3</sub>/SiO<sub>2</sub>、K<sub>2</sub>O/Na<sub>2</sub>O、Al<sub>2</sub>O<sub>3</sub>/(CaO+Na<sub>2</sub>O)等各项数值对于碎屑岩物源区及其构造背景判别最具判别性(表7),随SiO<sub>2</sub>含量的

增加,TFe<sub>2</sub>O<sub>3</sub>、MgO含量逐渐减少,呈现较好的负相关性。通过与大洋岛弧、大陆岛弧、活动大陆边缘、被动大陆边缘各项主量元素特征数值比较,研究区直罗组砂岩中主量元素特征除SiO<sub>2</sub>与大陆岛弧比较相近外,其他特征与活动大陆边缘最为契合。

利用碎屑岩地球化学特征及相应图解来还原源区构造环境方法被广泛应用(Absar et al., 2009; 许中杰等, 2013; 陶瑞等, 2019)。Roser and Korsch(1986, 1988)在研究新西兰古生代浊积岩时,建立了K<sub>2</sub>O/Na<sub>2</sub>O-SiO<sub>2</sub>双变量图解用于判别不同板块构造环境下形成的砂岩。将研究区直罗组样品进行

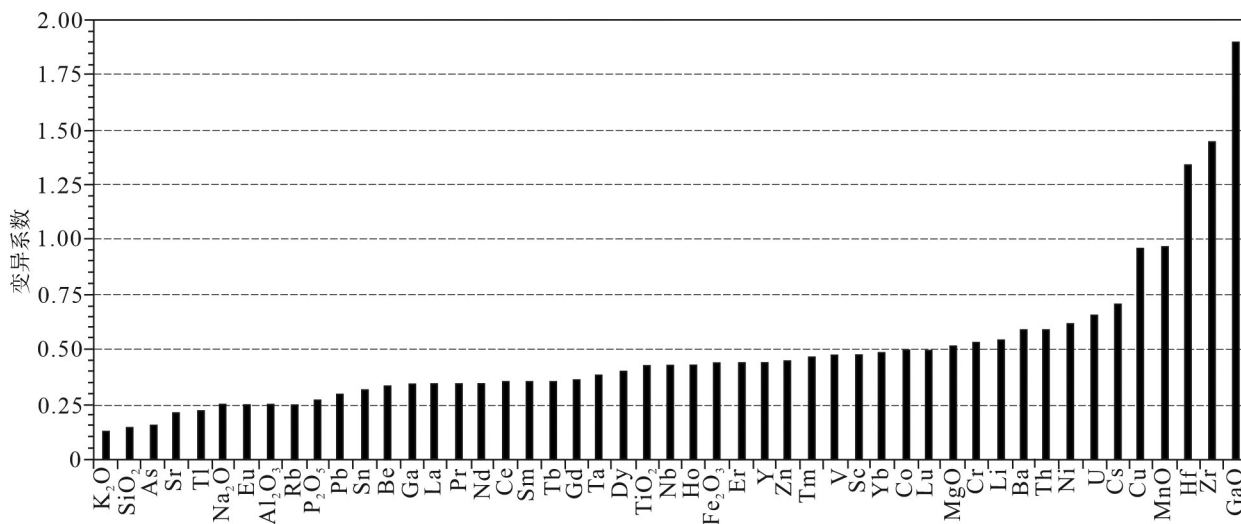


图6 灵武直罗组沉积物元素变异系数排序图

Fig.6 Sequence diagram of element differentiation coefficient in sediments of Zhiluo Formation in Lingwu

表6 灵武直罗组沉积物各元素特征参数统计

Table 6 Statistics of characteristic parameters of elements in sediments of Zhiluo Formation in Lingwu

元素	样品数	最小值	最大值	标准离差S	富集系数K	变异系数C
SiO <sub>2</sub>	16	43.66	75.3	9.14	0.97	0.14
TiO <sub>2</sub>	16	0.29	1.25	0.277	0.66	0.42
Al <sub>2</sub> O <sub>3</sub>	16	9.72	21.04	3.65	1.01	0.25
Fe <sub>2</sub> O <sub>3</sub>	16	1.76	8.44	1.99	1.91	0.43
MnO	16	0.03	0.43	0.098	0.1	0.97
MgO	16	0.7	3.05	0.77	1.01	0.51
CaO	16	0.42	19.07	4.59	1.4	1.9
Na <sub>2</sub> O	16	1.04	2.65	0.49	0.71	0.24
K <sub>2</sub> O	16	1.86	3.14	0.31	0.79	0.12
P <sub>2</sub> O <sub>5</sub>	16	0.04	0.11	0.019	0.07	0.27
LOI	16	2.1	16.39	3.585	4.67	0.77
Rb	16	67.6	150	23.9	0.87	0.25
Sr	16	165	377	49	1.04	0.21
Ba	16	435	2183	409	1.12	0.58
Th	16	4.6	23.1	6.1	0.97	0.58
U	16	1.1	10.1	2.6	1.77	0.65
Nb	16	5.4	19	4.6	0.73	0.42
Ta	16	0.4	1.29	0.29	0.75	0.38
Zr	16	98	1859	424	1.47	1.44
Hf	16	2.6	41.8	9.4	1.24	1.33
Co	16	6.4	29.8	5.9	1.22	0.49
Ni	16	10.1	53.4	13.4	0.87	0.61
Cr	16	20.7	83.8	24.1	0.99	0.53
V	16	39	139	34.7	1.07	0.47
Sc	16	5.1	19.7	5.1	1.11	0.47
Li	16	15.1	61.3	18	1.44	0.54
Cs	16	1.6	8.6	2.5	0.78	0.7
Be	16	1.2	3.4	0.6	0.84	0.33
Ga	16	12.2	27.2	5.7	0.9	0.33
Tl	16	0.4	0.9	0.14	0.97	0.22
Cu	16	4	42.6	13.9	0.85	0.96
Pb	16	12.8	32.3	5.5	1	0.29
Zn	16	31.5	107	26.6	0.88	0.44
As	16	2.6	3.9	0.5	0.71	0.15
Sn	16	1.4	3.4	0.7	0.98	0.31
La	16	18.6	60.9	11.7	0.85	0.34
Ce	16	44.7	137	24.6	0.93	0.35
Pr	16	4.5	13.9	2.6	0.9	0.34
Nd	16	16.7	51.4	9.7	0.84	0.34
Sm	16	3	8.9	1.8	0.85	0.35
Eu	16	0.8	1.6	0.3	0.89	0.24
Gd	16	2.3	7.3	1.5	0.85	0.36
Tb	16	0.37	1.08	0.22	0.78	0.35
Dy	16	2	6.9	1.5	0.74	0.4
Ho	16	0	1	0	0.7	0.42
Er	16	1.1	4.4	0.9	0.73	0.43
Tm	16	0.17	0.72	0.15	0.77	0.46
Yb	16	1.1	5	1	0.82	0.48
Lu	16	0.17	0.81	0.16	0.89	0.49
Y	16	9.6	41.1	8.7	0.97	0.43

注:主量元素单位为%,微量元素、稀土元素单位为 $10^{-6}$ 。

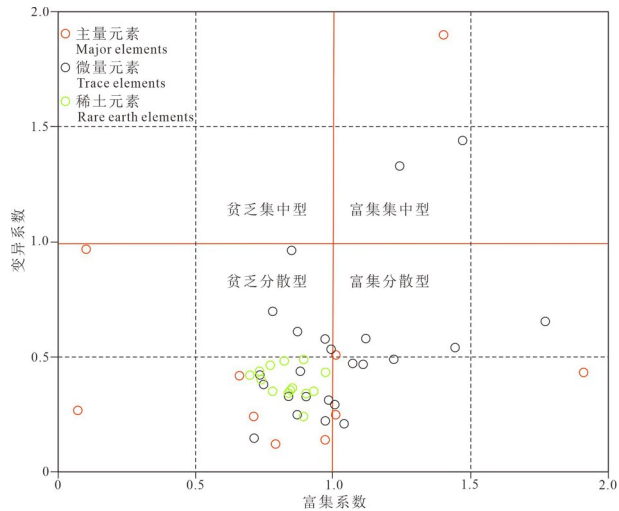


图7 灵武直罗组样品各元素富集系数及变异系数特征图  
Fig.7 Characteristics of enrichment coefficient and variation coefficient of various elements from Zhiluo group in Lingwu

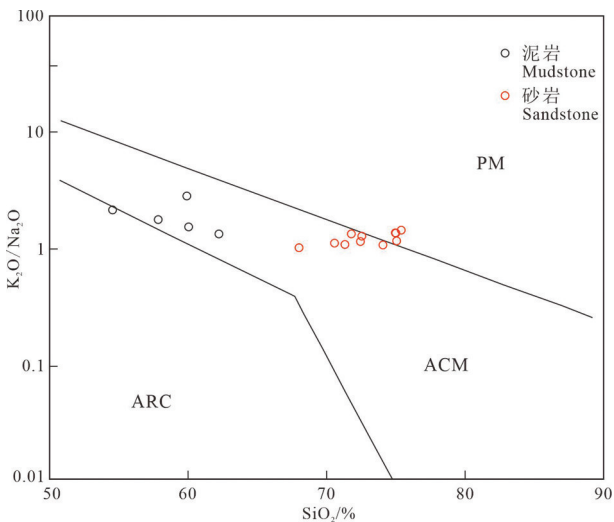


图8 灵武直罗组样品SiO<sub>2</sub>-K<sub>2</sub>O/Na<sub>2</sub>O构造环境判别图(据Roser and Korsch, 1986)

PM—被动大陆边缘; ACM—活动大陆边缘; ARC—大洋岛弧  
Fig.8 Tectonic setting discrimination diagram of SiO<sub>2</sub>-K<sub>2</sub>O/Na<sub>2</sub>O from the samples of Zhiluo Formation in Lingwu (after Roser and Korsch, 1986)  
PM—Passive continental margin; ACM—Active continental margin;  
ARC—Oceanic island arc

投图分析(图8),结果显示11件砂岩样品大多落入活动大陆边缘区域,有3件样品落入被动大陆边缘。Bhatia(1983)基于Fe、Ti、Mg在水-岩反应中的低活性建立了(TFe<sub>2</sub>O<sub>3</sub>+MgO)-TiO<sub>2</sub>、(TFe<sub>2</sub>O<sub>3</sub>+MgO)-Al<sub>2</sub>O<sub>3</sub>/SiO<sub>2</sub>构造环境判别图,对研究区直罗

表7 灵武直罗组砂岩与不同构造背景砂岩主量元素特征数值比较

Table 7 Comparison of major element characteristics between sandstone of Zhiluo Formation in Lingwu and sandstone of different structural backgrounds

构造背景	SiO <sub>2</sub> /%	TiO <sub>2</sub> /%	(TFe <sub>2</sub> O <sub>3</sub> +MgO)/%	Al <sub>2</sub> O <sub>3</sub> /SiO <sub>2</sub>	K <sub>2</sub> O/Na <sub>2</sub> O	Al <sub>2</sub> O <sub>3</sub> /(CaO+Na <sub>2</sub> O)
直罗组	69.92	0.54	4.58	0.18	1.17	3.14
大洋岛弧	58.83	1.06	11.7	0.29	0.39	1.72
大陆岛弧	70.69	0.64	6.79	0.2	0.61	2.42
活动大陆边缘	73.86	0.46	4.63	0.18	0.99	2.56
被动大陆边缘	81.95	0.49	2.89	0.1	1.6	4.15

组样品投图分析,砂岩样品投点大致集中于活动大陆边缘(图9),个别样品受主量元素本身稳定性及蚀变影响,出现分散现象。

Bhatia(1985)将4种不同构造环境(大洋岛弧、大陆岛弧、活动大陆边缘、被动大陆边缘)稀土元素特征归纳为:大洋岛弧,源区为未切割的岩浆弧,显示稀土总量低,弱轻稀土富集以及基本无Eu的负异常;大陆岛弧,源区为切割的岩浆弧,显示稀土总量较高、轻稀土中等富集以及弱的Eu负异常;活动大陆边缘和被动大陆边缘,其源区分别为上隆的基底及克拉通内部构造高地,且具有高稀土总量、高轻稀土富集以及较为明显的Eu负异常。同构造背景之下的泥岩和砂岩,泥岩的ΣREE含量比杂砂岩的高20%左右,故可以用泥岩稀土元素特征参数除以1.2作为同沉积期杂砂岩的对应参数值,该校正后的

稀土元素参数值可直接与Bhatia(1985)总结的4种构造环境下的杂砂岩稀土元素特征参数进行对比。通过稀土元素特征参数的综合对比分析发现(表8),研究区直罗组泥岩、砂岩稀土元素特征值均与活动大陆边缘背景下的稀土元素特征值最为相似,并且物源来自上隆的基底。

研究发现风化、成岩及蚀变作用对稀土元素的组成影响很弱,物源区岩石成分对稀土元素组成影响显著,故认为稀土元素组成可代表物源区源岩的稀土特征(Taylor and McLennan, 1985)。因此,沉积岩的稀土元素特征对物源区岩石地球化学特征及构造环境具有重要的指示意义(Taylor and McLennan, 1985; Cullers et al., 1988; McLennan and Taylor, 1991),La/Yb比值与ΣREE含量的变化关系可以反映某些岩石大类的成因特征(Bhatia, 1985);

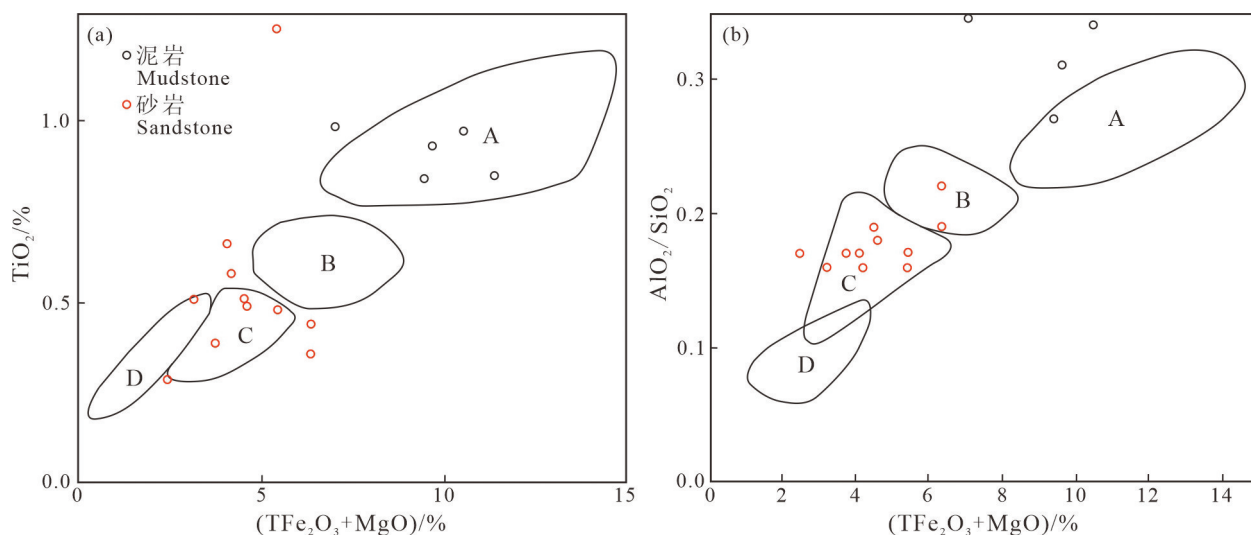


图9 灵武直罗组样品( $\text{TFe}_2\text{O}_3+\text{MgO}$ )— $\text{TiO}_2$ (a)和( $\text{TFe}_2\text{O}_3+\text{MgO}$ )— $\text{Al}_2\text{O}_3/\text{SiO}_2$ (b)构造环境判别图(据Bhatia, 1983)  
A—大洋岛弧; B—大陆岛弧; C—活动大陆边缘; D—被动大陆边缘

Fig.9 Tectonic setting discrimination diagrams of ( $\text{TFe}_2\text{O}_3+\text{MgO}$ )— $\text{TiO}_2$  (a) and ( $\text{TFe}_2\text{O}_3+\text{MgO}$ )— $\text{Al}_2\text{O}_3/\text{SiO}_2$  (b) of the samples from Zhiluo Formation in Lingwu (after Bhatia, 1983)

A—Oceanic island arc; B—Continental island arc; C—Active continental margin; D—Passive continental margin

表8 不同构造背景稀土元素特征值  
Table 8 REE value of different tectonic settings

构造背景	源区类型	La	Ce	$\Sigma$ REE	LREE/HREE	La/Yb	$(La/Yb)_N$	$\delta_{Eu}$
大洋岛弧	未切割的岩浆弧	8(1.7)	19(3.7)	58(10)	3.8(0.9)	4.2(1.3)	2.8(0.9)	1.04(0.11)
大陆岛弧	切割的岩浆弧	27(4.5)	59(8.2)	146(20)	7.7(1.7)	11(3.6)	7.5(2.5)	0.79(0.13)
活动大陆边缘	上隆的基底	37	78	186	9.1	12.5	8.5	0.6
被动大陆边缘	克拉通内部构造高地	39	85	210	8.5	15.9	8.5	0.56
直罗组泥岩平均值		44.06	87.8	204.4	10.1	15.63	11.21	0.7
泥岩校正后REE及比值		36.72	73.17	170.3	8.42	13.03	9.34	0.58
直罗组砂岩平均值		29.65	63.23	141.9	11.12	17.44	12.51	0.77

注:稀土元素单位为 $10^6$ ,括号内数据对应标准偏差;数据来自Bhatia, 1985, $(La/Yb)_N$ 采用球粒陨石标准化参数值计算。

La-Th-Sc、Th-Co-Hf/10和Th-Sc-Hf/10等图解可以进行源区构造环境的判别(Bhatia, 1983; Bhatia and Crook, 1986; Floyd and Leveridge, 1987; Shao et al., 2001)。利用这些判别图解的综合分析,可以对主量元素判别图解及稀土元素特征参数对比结果做进一步的补充和论证。

研究区直罗组沉积物样品微量、稀土元素在Ti/Zr-La/Sc图解中(图10)大多数落在活动大陆边缘区域,少量分散在大陆岛弧,部分泥岩样品落在活动大陆边缘区域上方。在La-Th-Sc图解中(图11a),

大多数泥岩样品比较一致地落在大陆岛弧区域内,砂岩样品集中于大陆岛弧区域上方。在Th-Co-Zr/10图解中(图11b),绝大多数样品落在大陆岛弧区域内及其周围。以上构造判别图解的分析表明,源区构造背景除主要与活动大陆边缘相关外,与大陆岛弧也有较多联系。这与区域上直罗组源区构造背景研究结果一致,同时也与华北陆缘显生宙以来大量的中酸性岩浆岩在时空上有很好的相容性。

笔者还通过对直罗组砂岩碎屑组分进行统计分析,并对样品进行投图,样品在Valloni and Maynard(1981)的QFL图解中主要落入活动陆缘消减带型区域(LE1)及周边,极少落入弧后盆地型(BA)和被动边缘型(TE)(图12a),在Crook(1974)QFR图中的点落入非稳定性的安第斯型活动边缘区(图12b)。分析结果说明源区构造属于不稳定的活动大陆边缘,且属于安第斯型活动大陆边缘,这与上述地球化学特征显示的结果是一致的。

综上分析,通过对灵武直罗组沉积物源区构造环境判别,总体显示为活动大陆边缘或活动陆缘消减带,而且可能为安第斯型活动大陆边缘。

## 6 结 论

(1)灵武直罗组碎屑岩元素地球化学基本特征分析表明,主量元素间相关系数较低,微量元素及稀土元素自身相关系数较高,Al<sub>2</sub>O<sub>3</sub>与微量元素Co、Ni、Cr、V、Sc、Li、Cs、Be、Ga、Tl、Cu、Pb、Zn、Sn等元素之间相关系数多大于0.9,TiO<sub>2</sub>与Nb之间的相关系数为0.98,整体显示了沉积物源以陆源碎屑为主;富集集中型( $K>1, C_v>1$ )元素有Zr、U、CaO元素;富集分散型( $K>1, C_v<1$ )元素有Al<sub>2</sub>O<sub>3</sub>、Fe<sub>2</sub>O<sub>3</sub>、MgO、Sr、Ba、U、Co、V、Sc、Li、Pb;贫乏分散型( $K<1, C_v<1$ )元

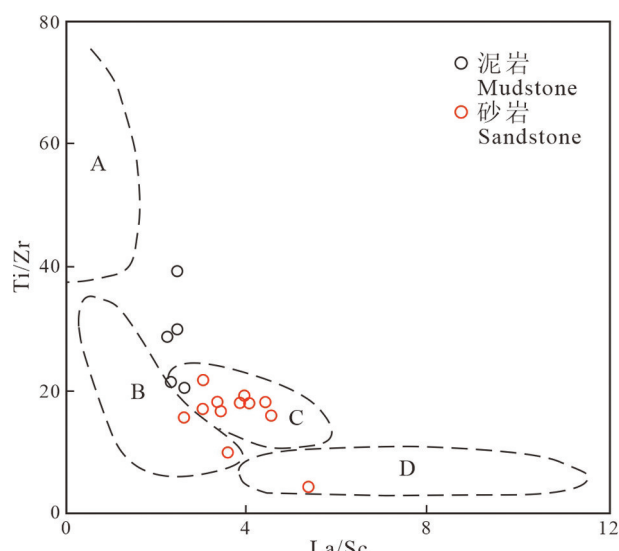


图10 灵武直罗组样品Ti/Zr-La/Sc构造环境判别图(据Bhatia and Crook, 1986)

A—大洋岛弧;B—大陆岛弧;C—活动大陆边缘;D—被动大陆边缘  
Fig.10 Tectonic setting discrimination diagram of La/Sc-Ti/Zr of the samples from Zhiluo Formation in Lingwu (after Bhatia and Crook, 1986)

A—Oceanic island arc; B—Continental island arc; C—Active continental margin; D—Passive continental margin

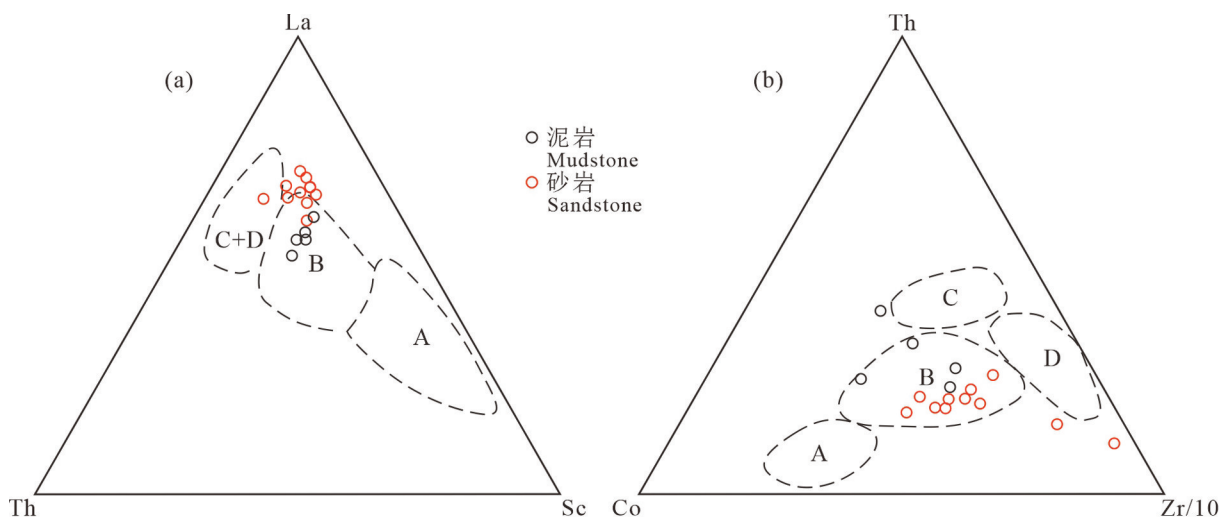


图11 灵武直罗组样品La-Th-Sc(a)和Th-Co-Zr/10(b)构造环境判别图(据Bhatia and Crook, 1986)  
A—大洋岛弧; B—大陆岛弧; C—活动大陆边缘; D—被动大陆边缘

Fig.11 Tectonic setting discrimination diagram of La-Th-Sc (a) and Th-Co-Zr/10 (b) of the samples from Zhiluo Formation in Lingwu (after Bhatia and Crook, 1986)

A—Oceanic island arc; B—Continental island arc; C—Active continental margin; D—Passive continental margin

素有  $\text{SiO}_2$ 、 $\text{TiO}_2$ 、 $\text{MnO}$ 、 $\text{Na}_2\text{O}$ 、 $\text{K}_2\text{O}$ 、 $\text{P}_2\text{O}_5$ 、 $\text{Rb}$ 、 $\text{Th}$ 、 $\text{Nb}$ 、 $\text{Ta}$ 、 $\text{Ni}$ 、 $\text{Cr}$ 、 $\text{Cs}$ 、 $\text{Be}$ 、 $\text{Ga}$ 、 $\text{Tl}$ 、 $\text{Cu}$ 、 $\text{Zn}$ 、 $\text{As}$ 、 $\text{Sn}$  及稀土元素; 缺乏贫乏集中型( $K<1$ ,  $C_V>1$ )元素。

(2) 灵武直罗组碎屑岩主量元素分析结果显示

泥岩主量元素与澳大利亚后太古宙平均页岩 PAAS 相似及沉积物源岩有酸性岩存在。泥岩 CIA=70.76~81.88, 砂岩的 ICV=1.02~1.6, 泥岩的 ICV=0.7~1.14。整体显示出砂岩 ICV>泥岩 ICV 且泥岩

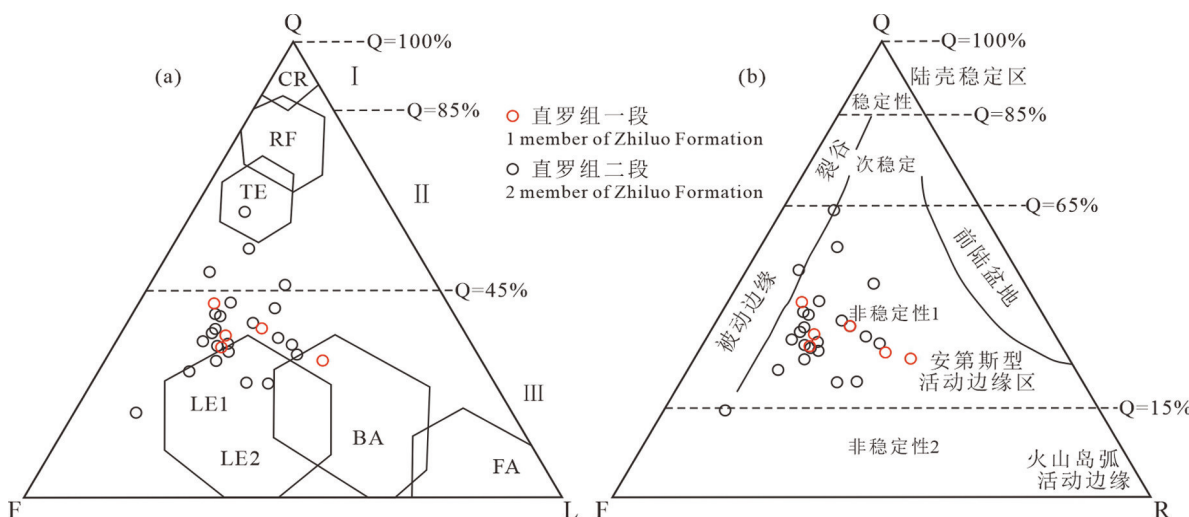


图12 灵武直罗组样品QFL与QFR图解(a, 据Valloni and Maynard, 1981; b, 据Crook, 1974)  
Q—单晶石英; F—单晶长石; L—不稳定岩屑; R—岩屑(包括多晶石英碎屑); CR—稳定克拉通内浅海盆地型; RF—裂谷及断陷盆地型;  
TE—被动边缘型; LE1—活动边缘消减带型; LE2—活动边缘转换断层型; BA—弧后盆地型; FA—弧前盆地型

Fig.12 QFL and QFR diagrams of the samples from Zhiluo Formation in Lingwu (a, after Valloni and Maynard, 1981;  
b, after Crook, 1974)

Q—Single crystal quartz; F—Single crystal feldspar; L—Unstable debris; R—Debris (including polycrystalline quartz debris); CR—Stable intracratonic shallow basin type; RF—Rift and fault basin type; TE—Passive margin type; LE1—Active continental margin subduction zone type; LE2—Active margin transform fault type; BA—Back-arc basin type; FA—Fore-arc basin type

ICV基本等于或小于1的特点,指示灵武直罗组没有经历或者经历了很弱的再旋回作用,属于构造活动背景下的初次沉积,分化程度中等。

(3)灵武直罗组碎屑岩主量、微量元素特征及 $Ti/Zr-La/Sc$ 、 $La-Th-Sc$ 、 $Th-Co-Zr/10$ 、QFL、QFR等图解投图分析表明,灵武直罗组源区构造背景主要与活动大陆边缘相关,与大陆岛弧也有较多联系,总体显示为活动大陆边缘或活动陆缘消减带,而且可能为安第斯型活动大陆边缘。

**致谢:**感谢四川省地质矿产勘查开发局区域地质调查队游水生高级工程师、李振江高级工程师在野外地质调查及论文编写过程中给予的大力支持与帮助。

## References

- Absar N, Raza M, Roy M, Naqvi S M, Roy A K. 2009. Composition and weathering conditions of Paleoproterozoic upper crust of Bundelkhand craton, Central India: Records from geochemistry of clastic sediments of 1.9 Ga Gwalior Group[J]. *Precambrian Research*, 168(3/4): 313–329.
- Bai Daoyuan, Zhou Liang, Wang Xianhui, Zhang Xiaoyang, Ma Tieqiu. 2007. Geochemistry of Nanhua–Cambrian sandstones in southeastern Hunan, and its constraints on Neoproterozoic–Early Paleozoic tectonic setting of South China[J]. *Acta Geologica Sinica*, 81(6): 755–771 (in Chinese with English abstract).
- Bhatia M R. 1983. Plate tectonics and geochemical composition of sandstones[J]. *The Journal of Geology*, 91(6): 611–627.
- Bhatia M R. 1985. Rare earth element geochemistry of Australian Paleozoic graywackes and mudrocks: Province and tectonic control[J]. *Sedimentary Geology*, 45: 97–113.
- Bhatia M R, Crook K A. 1986. Trace element characteristics of graywackes and tectonic setting discrimination of sedimentary basins[J]. *Contributions to Mineralogy and Petrology*, 92(2): 181–193.
- Cao Daiyong, Xu Hao, Liu Kang, Wei Yingchun, Zhang Wenfeng, Wang Xinguo. 2015. Coalfield tectonic evolution and its controlling factors at the western margin of Ordos Basin[J]. *Chinese Journal of Geology*, 50(2): 410–427 (in Chinese with English abstract).
- Chen Yin, Feng Xiaoxi, Chen Lulu, Jin Ruoshi, Miao Peisen, Sima Xianzhang, Miao Aisheng, Tang Chao, Wang Gui, Liu Zhongren. 2017. An analysis of U–Pb dating of detrital zircons and modes of occurrence of uranium minerals in the Zhiluo Formation of northeastern Ordos Basin and their indication to uranium sources[J]. *Geology in China*, 44(6): 1190–1206 (in Chinese with English abstract).
- Condie K C. 1993. Chemical composition and evolution of the upper continental crust: Contrasting results from surface samples and shales[J]. *Chemical Geology*, 104(1/4): 1–37.
- Cox R, Lowe D R, Cullers R L. 1995. The influence of sediment recycling and basement composition on evolution of mudrock chemistry in the southwestern United States[J]. *Geochimica et Cosmochimica Acta*, 59(14): 2919–2940.
- Crook K A W. 1974. Lithogenesis and geotectonics: The significance of compositional variation in flysch arenites (graywackes) [C]// Sepm Society for Sedimentary Geology: Tulsa, OK, USA, 304–310.
- Cullers R L, Basu A, Suttner L J. 1988. Geochemical signature of provenance in sand-size mineral in soil and stream near the tobacco root batholiths, Montana, USA[J]. *Chemical Geology*, 70: 335–348.
- Fedo C M, Nesbitt H W, Young G M. 1995. Unraveling the effects of potassium metasomatism in sedimentary rocks and paleosols, with implications for paleoweathering conditions and provenance[J]. *Geology*, 23(10): 921–924.
- Floyd P A, Leveridge B E. 1987. Tectonic environment of the Devonian Gramscatho Basin, South Cornwall: Framework mode and geochemical evidence from Turbiditic sandstones[J]. *Journal of the Geological Society*, 144(4): 531–542.
- Garzanti E, Padoan M, Setti M, Najman Y, Peruta L, Villa I M. 2013. Weathering geochemistry and Sr–Nd fingerprints of equatorial upper Nile and Congo muds[J]. *Geochemistry Geophysics Geosystems*, 14(2): 292–316.
- Geological Survey Institute of Ningxia Hui Autonomous Region. 2017. “China Regional Geology. Ningxia Zhi” [M]. Beijing: Geological Publishing House, 236–240 (in Chinese).
- Gromet L P, Haskin L A, Korotev R L, Dymek R F. 1984. The “north american shale composite”: Its compilation, major and trace element characteristics[J]. *Geochimica et Cosmochimica Acta*, 48(12): 2469–2482.
- Guo Hu, Chen Lulu, Tang Chao, Zhou Hongying, Zhu Qiang, SiMa Xianzhang, Yu Rengan. 2019. New recognition on the relationship between selenium-bearing minerals and uranium enrichment in Zhiluo Formation of Huangling area, Ordos Basin[J]. *Geology in China*, 46(1): 207–208 (in Chinese with English abstract).
- He Jingwen, Zhu Wenbin, Zheng Bihai, Wu Hailin, Ge Rongfeng, Luo Meng. 2015. Provenance of Sinian Sugetbrak sedimentary rocks in the Aksu area, NW Tarim: Evidence from detrital zircon geochronology[J]. *Acta Geological Sinica*, 89(1): 149–162 (in Chinese with English abstract).
- Jin Ruoshi, Feng Xiaoxi, Teng Xueming, Nie Fengjun, Cao Haiyang, Hou Huiqun, Liu Hongxu, Miao Peisen, Zhao Hualei, Chen Lulu, Zhu Qiang, Zhou Xiaoxi. 2020. Genesis of green sandstone/mudstone from Middle Jurassic Zhiluo Formation in the Dongsheng Uranium Orefield, Ordos Basin and its enlightenment

- for uranium mineralization[J]. *China Geology*, 3: 52–66.
- Kamp P C V D, Leake B E. 1985. Petrography and geochemistry of feldspathic and mafic sediments of the northeastern Pacific margin[J]. *Transactions of the Royal Society of Edinburgh Earth Sciences*, 76(4): 411–449.
- Lei Kaiyu. 2016. Comparative Research on Sedimentary Characteristics and Provenance of Zhiluo Formation in the Northern Ordos Basin and Southern Ordos Basin[D]. Xi'an: Northwest University (in Chinese with English abstract).
- Li Zhiming, Liu Jiajun, Hu Ruizhong, Liu Yuping, Li Chaoyang, He Mingqin. 2003. Tectonic setting and provenance of source rock for sedimentary rocks in Lanping Mesozoic–Cenozoic Basin: Evidences from geochemistry of sandstones[J]. *Acta Sedimentologica Sinica*, 21(4): 547–552 (in Chinese with English abstract).
- Long Xiaoping, Yuan Chao, Sun Ming, Xiao Wenjiao, Lin Shoufa, Wang MingJing, Cai Keda. 2008. Geochemical characteristics and sedimentary environments of Devonian low metamorphic clastic sedimentary rocks in the southern margin of the Chinese Altai, North Xinjiang[J]. *Acta Petrologica Sinica*, 24(4): 718–731 (in Chinese with English abstract).
- Luo Wei, Liu Chiyan, Zhang Dongdong, Wang Jianqiang, Niu Haiqing, Guo Pei. 2016. Geochemistry characteristics of the Middle Jurassic Zhiluo Formation in Helan Mountain–Liupan Mountain area[J]. *Acta Geologica Sinica*, 18(6): 1030–1043 (in Chinese with English abstract).
- McLennan S M, Taylor S R. 1991. Sedimentary rocks and crustal evolution: Tectonic setting and secular trends[J]. *The Journal of Geology*, 99(1): 1–21.
- McLennan S M, Hemming S, McDaniel D K, Hanson G N. 1993. Geochemical approaches to sedimentation, provenance, and tectonics[J]. *Geological Society of America Special Papers*, 284: 21–40.
- Miao Zongli, Zhu Lijuan, Hou Mingcai, Chen Anqing, Luo Wen, Shi Xin, Wang Haihong, Liu Yicang, Wang Lianguo, Hou Changbing, Guo Xiaojun, Guo Jinzhe, Shao Xiaoyan. 2018. Sedimentary facies of Middle Jurassic Zhiluo Formation in Yanwu area, Ordos Basin[J]. *Journal of Chengdu University of Technology (Natural Science Edition)*, 45(2): 166–176 (in Chinese with English abstract).
- Nesbitt H W. 1979. Mobility and fractionation of rare earth elements during weathering of a granodiorite[J]. *Nature*, 279: 206–210.
- Nesbitt H W, Young G M. 1982. Early Proterozoic climates and plate motions inferred from major element chemistry of lutites[J]. *Nature*, 299(5885): 715–717.
- Nesbitt H W, MacRae N D, Kronberg B I. 1990. Amazon deep-sea fan muds: Light REE enriched products of extreme chemical weathering[J]. *Earth and Planetary Science Letters*, 100: 118–123.
- Nesbitt H W, Young G M, McLennan S M, Keays R R. 1996. Effects of chemical weathering and sorting on the petrogenesis of siliciclastic sediments, with implications for provenance studies[J]. *Journal of Geology*, 104(5): 525–542.
- Roser B P, Korsch R J. 1986. Determination of tectonic setting of sandstone–mudstone suites using content and ratio[J]. *The Journal of Geology*, 94(5): 635–650.
- Roser B P, Korsch R J. 1988. Provenance signatures of sandstone–mudstone suites determined using discriminant function analysis of major-element data[J]. *Chemical Geology*, 67(1): 119–139.
- Shao L, Stattegger K, Garbe-Schoenberg C. 2001. Sandstone petrology and geochemistry of the Turpan Basin (NW China): Implications for the tectonic evolution of a continental basin[J]. *Journal of Sedimentary Research*, 71(1): 37–49.
- Song Fang, Niu Zhijun, He Yaoyan, Yang Wengqiang. 2016. U–Pb age of detrital zircon and its restriction of provenance paleogeographic characteristics of Early Nanhu Period in Middle Yangzi[J]. *Acta Geologica Sinica*, 90(10): 2661–2680 (in Chinese with English abstract).
- Su Benxun, Chen Yuelong, Liu Fei, Wang Qiaoyun, Zhang Hongfei, Lan Zhongwu. 2006. Geochemical characteristics and significance of Triassic sandstones of Songpan–Ganzi block[J]. *Acta Petrologica Sinica*, 22(4): 961–970 (in Chinese with English abstract).
- Sun Lixing, Zhang Yun, Zhang Tianfu, Cheng Yinhang, Li Yanfeng, Ma Hailin, Yang Cai, Guo Jiacheng, Lu Chao, Zhou Xiaoguang. 2017. Jurassic sporopollen of Yan'an Formation and Zhiluo Formation in the northeastern Ordos Basin, Inner Mongolia, and its paleoclimatic significance[J]. *Earth Science Frontiers*, 24(1): 32–47 (in Chinese with English abstract).
- Sun S S, McDonough W F. 1989. Chemical and isotopic systematics of oceanic basalts: Implications for mantle compositions and processes[J]. *Geological Society London Special Publications*, 42: 313–345.
- Tao Rui, Deng Jianghong, Wang Chunlin, Gong Tingting. 2019. New understanding of the Devonian Wenquan Formation in Fengqing, western Yunnan[J]. *Journal of Stratigraphy*, 43(1): 63–73 (in Chinese with English abstract).
- Taylor S R, McLennan S M. 1985. The Continental Crust: Its Composition and Evolution[M]. Oxford: Blackwell, 312.
- Valloni R, Maynard J B. 1981. Detrital modes of recent deep-sea sands and their relation to tectonic setting: A first approximation[J]. *Sedimentology*, 28: 75–83.
- Wronkiewicz D J, Condé K C. 1989. Geochemistry and provenance of sediments from the Pongola Supergroup, South Africa: Evidence for a 3.0–Ga-old continental craton[J]. *Geochimica et Cosmochimica Acta*, 53(7): 1537–1549.
- Wu Sujuan, Zhang Yongsheng, Xing Enyuan. 2016. Geochemistry of Ordovician detrital rocks and its constraints on provenance in Zhuozishan area, Northwest Ordos Basin[J]. *Acta Geologica*

- Sinica, 90(8): 1860–1873 (in Chinese with English abstract).
- Wu Zhaojian, Han Xiaozhong, Yi Chao, Qi Caiji, Hui Xiaochao, Wang Mingtai. 2013. Geochemistry of sandstones from the Middle Jurassic Zhiluo Formation, Dongsheng District, Northeastern Ordos Basin: Implications for provenance and tectonic setting[J]. Geoscience, 27(3): 557–567 (in Chinese with English abstract).
- Xu Daliang, Liu Hao, Wei Yunxu, Peng Lianhong, Deng Xing. 2016. Detrital zircon U–Pb dating of Zhengjiaya Formation from the Shengnongjia area in the Northern Yangtze Block and its tectonic implications[J]. Acta Geologica Sinica, 90(10): 2648–2660 (in Chinese with English abstract).
- Xu Zhongjie, Cheng Rihui, Wang Liaoliang, Zhang Li, Shen Yanjie, Yu Zhengfeng. 2013. Mineralogical and element geochemical characteristics of the Late Triassic–Middle Jurassic sedimentary rocks in southwestern Fujian Province: Constraints on changes of basin tectonic settings[J]. Acta Petrologica Sinica, 29(8): 2913–2924 (in Chinese with English abstract).
- Xue Rui, Zhao Junfeng, Yan Zhandong, Yang Yao, Zhao Xudong, Zhao Zhongping. 2017. Sedimentary characteristics and evolution of the Jurassic Zhiluo Formation in northern Ordos Basin[J]. Journal of Palaeogeography, 19(6): 999–1012 (in Chinese with English abstract).
- Yang Jun, Wang Shanbo, Liu Fei. 2019. Sedimentary facies of the Zhiluo Formation and its relationship with uranium mineralization in the Huanxian area, west of Ordos Basin[J]. Science Technology and Engineering, 19(17): 64–70 (in Chinese with English abstract).
- Yi Chao, Han Xiaozhong, Li Xide, Zhang Kang, Chen Xinlu. 2014. Study on sandstone petrologic feature of the Zhiluo Formation and its controls on uranium mineralization in northeastern Ordos Basin[J]. Geological Journal of China Universities, 20(2): 185–197 (in Chinese with English abstract).
- Zhang Bin, Liu Hongxu, Yi Chao, Ding Bo, Zhang Yan. 2020. Petrogeochemical characteristics and provenance indication of the sandstone from lower submember, lower member of Zhiluo Formation in Nalinggou Area, Northern Ordos Basin[J]. Uranium Geology, 36(2): 84–95 (in Chinese with English abstract).
- Zhang Long, Wu Bailin, Liu Chiyang, Lei Kaiyu, Hou Huiqun, Sun Li, Cun Xiaoni, Wang Jianqiang. 2016. Provenance analysis of the Zhiluo Formation in the sandstone-hosted uranium deposits of the Northern Ordos Basin and implications for uranium mineralization[J]. Acta Geologica Sinica, 90(12): 3441–3453 (in Chinese with English abstract).
- Zhang Tianfu, Sun Lixing, Zhang Yun, Cheng Yinhang, Li Yanfeng, Ma Hailin, Lu Chao, Yang Cai, Guo Gengwan. 2016. Geochemical characteristics of the Jurassic Yan'an and Zhiluo Formations in the northern margin of Ordos Basin and their paleoenvironmental implications[J]. Acta Geologica Sinica, 90(12): 3454–3472 (in Chinese with English abstract).
- Zhang Yan, Yi Chao. 2017. Inversion method of physical properties of optimized logging interpretation in Ordos Basin application of Zhiluo Formation in the northern area[J]. Journal of Minerals, (Supp.): 280–281 (in Chinese with English abstract).
- Zhang Yun, Zhang Tianfu, Cheng Xianyu, Sun Lixin, Cheng Yinhang, Wang Shaoyi, Wang Shanbo, Ma Hailin, Lu Chao. 2022. A brief analysis on the three-dimensional geological structure and uranium mineralization of Jurassic uranium-bearing rock series in the northeastern Ordos Basin[J]. Geology in China, 49(1): 66–80 (in Chinese with English abstract).
- Zhang Zilong, Han Xiaozhong, Li Shengxiang. 2008. Geochemical characteristics and uranium metallogenesis of sand bodies in Zhiluo Formation, Ordos Basin[J]. World Nuclear Geology, 25(2): 79–85 (in Chinese with English abstract).
- Zhang Zilong, Fan Honghai, Cai Yuqi, Zhao Xingqi, Liu Hongxu, He Feng, Li Ping, Yang Mengjia. 2016. The organic geochemical characteristics of the Zhiluo Formation and its relationship with uranium mineralization in the Huangling area, Ordos Basin[J]. Acta Geologica Sinica, 90(12): 3408–3423 (in Chinese with English abstract).
- Zhao Hualei, Chen Lulu, Feng Xiaoxi, Li Jianguo, Chen Yin, Wang Gui. 2018. Features of clay minerals in the Middle Jurassic Zhiluo Formation sandstones of the Nalinggou area in the Ordos Basin and a preliminary comparison with adjacent areas[J]. Geological Journal of China Universities, 24(5): 627–636 (in Chinese with English abstract).
- Zhao Junfeng, Liu Chiyang, Liang Jiwei, Wang Xiaomei, Yu Lin, Huang Lei, Liu Yongtao. 2010. Restoration of the origin sedimentary boundary of the Middle Jurassic Zhiluo Formation–Anding Formation in the Ordos Basin[J]. Acta Geologica Sinica, 84(2): 553–569 (in Chinese with English abstract).
- Zhao Lei. 2011. Sedimentary Characteristics and its Hydrogeological Significance of Jurassic Zhiluo Formation in the East of Ningxia Province[D]. Shandong: Shandong University of Science and Technology (in Chinese with English abstract).
- Zhao Yingli. 2010. Late Paleozoic Tectonic Evolution of the Central and Southern Great Xing'an Ranges: Constraints from Provenance Characteristics of Permian Sandstones[D]. Changchun: Jilin University (in Chinese with English abstract).
- Zhao Yingli, Liu Yongjiang, Han Guoqing, Wu Lina, Li Weimin, Wen Quanbo, Liang Chengyue. 2012. Geochemical characteristics of major elements in the Permian sandstones from the central and southern Great Xing'an Ranges and discriminations on their tectonic environment of the provenance[J]. Journal of Jilin University (Earth Science Edition), (S2): 285–297 (in Chinese with English abstract).

## 附中文参考文献

柏道远, 周亮, 王先辉, 张晓阳, 马铁球. 2007. 湘东南华南系—寒武系砂岩地球化学特征及对华南新元古代—早古生代构造背景的

- 制约[J]. 地质学报, 81(6): 755–771.
- 曹代勇, 徐浩, 刘亢, 魏迎春, 占文锋, 王信国. 2015. 鄂尔多斯盆地西缘煤田构造演化及其控制因素[J]. 地质科学, 50(2): 410–427.
- 陈印, 冯晓曦, 陈路路, 金若时, 苗培森, 司马献章, 苗爱生, 汤超, 王贵, 刘忠仁. 2017. 鄂尔多斯盆地东北部直罗组内碎屑锆石和铀矿物赋存形式简析及其对铀源的指示[J]. 中国地质, 44(6): 1190–1206.
- 郭虎, 陈路路, 汤超, 周红英, 朱强, 司马献章, 俞初安. 2019. 鄂尔多斯盆地黄陵地区直罗组含硒矿物与铀富集关系的新认识[J]. 中国地质, 46(1): 207–208.
- 何景文, 朱文斌, 郑碧海, 吴海林, 葛荣峰, 罗梦. 2015. 塔里木西北缘阿克苏地区震旦系苏盖特布拉克组沉积物源分析: 碎屑锆石年代学证据[J]. 地质学报, 89(1): 149–162.
- 雷开宇. 2016. 鄂尔多斯盆地北部和南部直罗组沉积—物源对比研究及其意义[D]. 西安: 西北大学.
- 李志明, 刘家军, 胡瑞忠, 刘玉平, 李朝阳, 何明勤. 2003. 兰坪中新生代盆地沉积岩源区构造背景和物源属性研究——砂岩地球化学证据[J]. 沉积学报, 21(4): 547–552.
- 龙晓平, 袁超, 孙敏, 肖文交, 林寿发, 王毓靖, 蔡克大. 2008. 北疆阿尔泰山缘泥盆系浅变质碎屑沉积岩地球化学特征及其形成环境[J]. 岩石学报, 24(4): 718–731.
- 罗伟, 刘池洋, 张东东, 王建强, 牛海青, 郭佩. 2016. 贺兰山一六盘山地区中侏罗统直罗组地球化学特征及其地质意义[J]. 古地理学报, 18(6): 1030–1043.
- 缪宗利, 朱莉娟, 侯明才, 陈安清, 罗文, 石鑫, 王海红, 刘一仓, 王联国, 侯长冰, 郭小军, 郭京蜇, 邵晓岩. 2018. 鄂尔多斯盆地演武地区中侏罗统直罗组沉积相[J]. 成都理工大学学报(自然科学版), 45(2): 166–176.
- 宁夏回族自治区地质调查院. 2017.《中国区域地质志·宁夏志》[M]. 北京: 地质出版社, 236–240.
- 宋芳, 牛志军, 何垚硯, 杨文强. 2016. 中扬子地区南华纪早期碎屑锆石 U-Pb 及其对物源特征和古地理格局的约束[J]. 地质学报, 90(10): 2661–2680.
- 苏本勋, 陈岳龙, 刘飞, 王巧云, 张宏飞, 兰中伍. 2006. 松潘—甘孜地块三叠系砂岩的地球化学特征及其意义[J]. 岩石学报, 22(4): 961–970.
- 孙立新, 张云, 张天福, 程银行, 李艳峰, 马海林, 杨才, 郭佳成, 鲁超, 周晓光. 2017. 鄂尔多斯北部侏罗纪延安组、直罗组孢粉化石及其古气候意义[J]. 地学前缘, 24(1): 32–47.
- 陶瑞, 邓江红, 王春林, 龚婷婷. 2019. 滇西凤庆习谦泥盆系温泉组地层新认识[J]. 地层学杂志, 43(1): 63–73.
- 吴素娟, 张永生, 邢恩袁. 2016. 桌子山地区奥陶系乌拉力克组碎屑岩地球化学特征及其对物源的制约[J]. 地质学报, 90(8): 1860–1873.
- 吴兆剑, 韩效忠, 易超, 祁才吉, 惠小朝, 王明太. 2013. 鄂尔多斯盆地东胜地区直罗组砂岩的地球化学特征与物源分析[J]. 现代地质, 27(3): 557–567.
- 徐大良, 刘浩, 魏运许, 彭练红, 邓新. 2016. 扬子北缘神农架地区郑家垭组碎屑锆石年代学及其构造意义[J]. 地质学报, 90(10): 2648–2660.
- 许中杰, 程日辉, 王嘹亮, 张莉, 沈艳杰, 于振锋. 2013. 闽西南地区晚三叠—中侏罗世沉积岩矿物和元素地球化学特征: 对盆地构造背景转变的约束[J]. 岩石学报, 29(8): 2913–2924.
- 薛锐, 赵俊峰, 同占冬, 杨瑶, 赵旭东, 赵中平. 2017. 鄂尔多斯盆地北部侏罗系直罗组沉积特征与演化[J]. 古地理学报, 19(6): 999–1012.
- 杨君, 王善博, 刘飞. 2019. 鄂尔多斯盆地西缘环县地区直罗组沉积相及其与铀矿化的关系[J]. 科学技术与工程, 19(17): 64–70.
- 易超, 韩效忠, 李西得, 张康, 陈心路. 2014. 鄂尔多斯盆地东北部直罗组砂岩岩石学特征与铀矿化关系研究[J]. 高校地质学报, 20(2): 185–197.
- 张宾, 刘红旭, 易超, 丁波, 张艳. 2020. 鄂尔多斯盆地北部纳岭沟地区直罗组下段下亚段砂岩岩石地球化学特征及对物源的指示[J]. 铀矿地质, 36(2): 84–95.
- 张龙, 吴柏林, 刘池洋, 雷开宇, 侯惠群, 孙莉, 寸小妮, 王建强. 2016. 鄂尔多斯盆地北部砂岩型铀矿直罗组物源分析及其铀成矿意义[J]. 地质学报, 90(12): 3441–3453.
- 张天福, 孙立新, 张云, 程银行, 李艳峰, 马海林, 鲁超, 杨才, 郭根万. 2016. 鄂尔多斯盆地北缘侏罗纪延安组、直罗组泥岩微量、稀土元素地球化学特征及其古沉积环境意义[J]. 地质学报, 90(12): 3454–3472.
- 张艳, 易超. 2017. 最优化测井解释物性反演方法在鄂尔多斯盆地北部地区直罗组中的应用[J]. 矿物学报, (增刊): 280–281.
- 张云, 张天福, 程先钰, 孙立新, 程银行, 王少铁, 王善博, 马海林, 鲁超. 2022. 鄂尔多斯盆地东北部侏罗纪含铀岩系三维地质结构与铀成矿规律浅析[J]. 中国地质, 49(1): 66–80.
- 张字龙, 韩效忠, 李胜祥. 2008. 鄂尔多斯盆地直罗组砂体地球化学特征及其铀成矿作用[J]. 世界核地质科学, 25(2): 79–85.
- 张字龙, 范洪海, 蔡煜琦, 赵齐兴, 刘红旭, 贺锋, 李平, 杨梦佳. 2016. 鄂尔多斯盆地黄陵地区直罗组有机地球化学特征及其与铀成矿关系[J]. 地质学报, 90(12): 3408–3423.
- 赵华雷, 陈路路, 冯晓曦, 李建国, 陈印, 王贵. 2018. 鄂尔多斯盆地纳岭沟地区直罗组砂岩粘土矿物特征及初步对比研究[J]. 高校地质学报, 24(5): 627–636.
- 赵俊峰, 刘池洋, 梁积伟, 王晓梅, 喻林, 黄雷, 刘永涛. 2010. 鄂尔多斯盆地直罗组—延安组沉积期原始边界恢复[J]. 地质学报, 84(4): 553–569.
- 赵蕾. 2011. 宁东地区侏罗系直罗组沉积特征及其水文地质意义[D]. 青岛: 山东科技大学.
- 赵英利. 2010. 大兴安岭中南部二叠纪砂岩物源分析对晚古生代区域构造演化的制约[D]. 长春: 吉林大学.
- 赵英利, 刘永江, 韩国卿, 吴琳娜, 李伟民, 温泉波, 梁琛岳. 2012. 大兴安岭中南段二叠纪砂岩主量元素地球化学特征及物源区构造环境的判别[J]. 吉林大学学报(地球科学版), 42(S2): 258–297.